



CloudSat inferred contrasting monsoon intra-seasonal variation in the cloud vertical structure over Indian regions

M. C. R. Kalapureddy^{1,2} · Sukanya Patra¹ · Vipul Dhavale¹ · Meenu R. Nair^{1,2}

Received: 13 June 2022 / Accepted: 15 December 2022 / Published online: 10 January 2023
© The Author(s), under exclusive licence to Springer-Verlag GmbH Germany, part of Springer Nature 2023

Abstract

Earlier studies reported the contrasting cloud properties over central India during intraseasonal oscillation of the Indian summer monsoon (ISM). This intraseasonal ISM variation in the cloud vertical structure (VSC) over different parts of India is yet to be explored. To fill this gap area, VSC derived from nine years of CloudSat measurements over geographically different but having homogenous ISM rainfall Indian regions are selected for the study. We investigated VSC, types of clouds, and microphysical properties during the intra-seasonal variation of ISM. Significant contrast was found in the mid-tropospheric cloud region during the ISM spells. Analysis of cloud types shows significant intra-seasonal variability with the presence or absence of mixed-phase clouds (As, Ns, and Ac). In ISM (active and break) spells, the core monsoon regions (CI, CE, WI) share similar VSC features (complete or void mid-levels). Hence, microphysical properties follow similar characteristics except for ice water content which differs profusely among them. Over these regions, ten times higher ice effective radius during active days indicates dominating ice process compared to break days. Larger-sized ice hydrometeors ($> 25 \mu\text{m}$) are present at 5–6 km, which shows good interrelation with the ISM active and break spells above freezing level, and its size decreases with altitude. Whereas no difference in VSC is found during different ISM spells over the eastern part of India (WB and EI) except in the ice microphysical parameters, which are more dominant during break days. Further, irregular and discontinuous VSC over North and South India (NI and SI) could be due to their pertinent geographical conditions. Suppression of cloud processes at mid-tropospheric altitude is one of the most important reasons behind reduced precipitation over the core ISM regions. Mid-tropospheric drying is a remarkable sign of ISM break, which is the main source of suppressed convection and cloud activity over the core ISM region. This CloudSat study brought robust composite cloud vertical structure for the ISM intra-seasonal variability of cloud over different regions of India to improve the understanding of cloud-related processes and then increase the predictive capabilities of large-scale models.

Abbreviations

ISM	Indian summer monsoon
As	Altostratus
Ns	Nimbostratus
Ac	Altostratus
CI	Central India
CE	Central East India
WI	West India
WB	West Bengal
EI	East India
NI	North India

NW	North-West India
SI	South India
WG _s	Western Ghats
Cu	Cumulus (including cumulus congestus)
Sc	Stratocumulus
Ns	Nimbostratus
Ac	Altostratus
As	Altostratus
St	Stratus
LWC	Liquid water content
IWC	Ice water content
IER	Ice effective radius
INC	Ice number concentration
CPR	Cloud Profiling Radar

✉ M. C. R. Kalapureddy
kalapureddy1@gmail.com

¹ Indian Institute of Tropical Meteorology (IITM), Dr.Homi Bhabha Road, Pashan, Pune 411008, India

² Department of Atmospheric and Space Sciences, Savtribai Phule Pune University, Pune 411007, India

1 Introduction

The Indian Summer Monsoon (ISM) forms the most dramatic monsoon system in the northern hemisphere. The ISM, also called the southwest monsoon (June–September), has been characterized by country-wide rainfall with a surface heat low and a trough of low pressure called monsoon trough. Surface heat low exists over northwest India and adjoining Pakistan. Monsoon trough stretches across the central plains of India towards Gangetic West Bengal and the adjoining north Bay of Bengal (BoB; Rao 1976; Krishnamurti and Bhalme 1976). Over the Indian latitude, a reversal of the vertical circulation occurs between the equatorial Indian Ocean and the adjacent Indian continent due to seasonal movement of the inter or continental tropical convergence zone (ITCZ/CTCZ) in boreal summer. Clearly, the space-time variation of CTCZ over the Indian subcontinent is linked with the monsoon variability (Gadgil 2018).

A convectively coupled monsoon intra-seasonal oscillation (MISO) describes the ISM in active and break ISM spells (Goswami and Xavier 2005). The active ISM period is identified by an unstable zonal flow and frequent formation of the synoptic-scale transient disturbances and, consequently, widespread rainfall all over India. On the contrary, the break ISM spell is characterized by the large-scale stability of the system. Since the monsoon trough lies close to the foothills of the Himalayas, and the formation of transient disturbances is absent, the ISM core region receives below normal rainfall. This ISM active-break cycle fluctuates on two super-synoptic scales of 10–20 days and 30–40 days (Krishnamurti and Bhalme 1976; Krishnamurti and Ardanuy 1980). Breaks in the ISM have an adverse impact on agriculture in India. An extended period of breaks in ISM in 2002 led to drought-like conditions (Rajeevan et al. 2010). Representation of mean monsoon circulation in climate models is very important to assess biases in future climate change projections (Gadgil and Sajani et al. 1998; Wang et al. 2004; Rajeevan and Nanjundiah 2009). Errors in the simulation of monsoon circulation probably result from inadequate representation and parameterization of the cloud. Cloud vertical structure (VSC) is a versatile parameter that indicates inherent connection among various altitudes through the change of cloud hydrometeor's type, macro- and micro-physical properties due to the varied processes associated with the temperature profile.

The radiative energy budget and the hydrological cycle of the Earth's atmosphere are based on the distribution of clouds. To encapsulate cloud effect on the hydrological cycle and radiative (incoming and outgoing) fluxes accurately in regional and global models, the interaction

between microphysical and dynamical processes going within the cloud needs to be well understood (Baker 1997). The VSC directly influences atmospheric circulation by changing the radiative cooling profile and the atmospheric static stability (Subrahmanyam and Kumar 2017; Zhang et al. 2014). Using the atmospheric models, Wang and Rossow (1998) reported the effect of VSC on atmospheric circulation. They showed that three important VSC parameters play a pivotal role. These are the presence of multiple layered clouds, the location of the uppermost cloud top, and the distance of separation between two successive layers in multi-layered cloud systems. It was also shown that in circulation strength, more than horizontal gradients, vertical gradients in the cloud distribution were more important in their model (Rind and Rossow 1984). Thus, it is essential to know the vertical distribution of the cloud and its areal cover. Accurately detailing the vertical distribution of cloud-optical properties contributes largely to the uncertainties in examining the radiative effects of clouds. The VSC is considered an important entity for better climate forecast and modeling that many studies have emphasized (e.g., Weare 2000; Zhang et al. 2010). Hence analyzing and extracting VSC from the measurements are important for a variety of reasons.

Earlier studies reported explaining large-scale rainfall and circulation features of ISM associated with the MISO (Webster et al. 1998; Goswami and Mohan 2001; Rao et al. 2009; Rajeevan et al. 2010). The important sub-grid scale cloud features are missed due to the lack of high-resolution datasets on the VSC measurements. Conventional passive-sensor satellite data provides accurate location and partially the vertical cloud extent, but it largely misses the finer details on the vertical distribution of cloud layers. The launching of the CloudSat mission provided an opportunity to study VSC globally. Some recent investigations explored the CloudSat data for different spatial and vertical distributions of clouds over the Indian region. CloudSat data was used by Jiang et al. (2011) for the years 2006–2009 to explore the variation of cloud water content (CWC) and cloud types associated with the northward propagation of MISO. This study concludes that while cloud Ice Water Content (IWC) at higher altitudes lags the convection, increased cloud Liquid Water Content (LWC) tends to appear north of maximum rainfall. It also discussed the transition between shallow cumuli, deep convection, and upper anvil clouds. Using the CloudSat five years dataset (2006–2010), Rajeevan et al. (2013) calculated the mean spatial distribution of cloud microphysical and VSC tilting properties over the central Indian region.

Das et al. (2013) studied the optical, radiative, macro-physical, and micro-physical properties of four types of clouds over the ISM core region. This study concluded that the cloud top and base height showed a bi-modal distribution. It also concluded that relative to the break

Table 1 Active and break spells of Indian Summer Monsoon chosen for the present study

Year	Active spell	Break spell
2008	27–29 July, 9–12 August	18–22 July, 15–17 August
2009	12–16 July, 19–23 July	29 July–10 August, 16–19 August
2010	1–3 August, 5–7 August	17–20 July
2011	9–12 August, 26–28 August	1–3 July
2012	11–13 August	–
2013	19–22 August	–
2014	19–23 July, 4–6 August	15–21 August
2015	25–29 July	13–15 July, 6–10 August, 20–25 August
2016	3–6 July, 9–12 July, 2–7 August	19–21 July

ISM, low-level and high-level clouds are higher during the active ISM. In contrast, sub-visible and thin high-level clouds are more frequent during the break ISM spell. Johansson et al. (2015) studied the vertical distribution of different clouds and their cloud radiative heating. This study concluded that the northward migration and monsoon retreat (May - October) are followed by cloud radiative heating. It was found that intense warming of the mid-troposphere occurs due to alto- and nimbostratus clouds, along with equally intense cooling of the upper troposphere. Significant radiative warming in the middle and upper troposphere occurs due to deep convective towers. However, strong cooling in the base and inside of the tropical tropopause layer is seen. During the active ISM, ample cooling of the surface is observed due to deep convective and stratiform clouds. On the contrary, high clouds contribute to twice the radiative warming effect during the active compared to the break ISM period.

However, the time resolution of such observations is low. This is because, for any particular location, the repeat time of these polar-orbiting satellites is very large (L'Ecuyer and Jiang 2011; Qian et al. 2012). All the studies mentioned above are based on the CloudSat-Calipso combined datasets for five or fewer years of data. It puts constraints on studying the VSC region-wise. Hence, to increase the number of data points for analysis, the regions under consideration are spatially large in all previous studies. Here we hypothesized that the change in cloud properties depends on the region under consideration. Hence to overcome this problem, we selected nine years long-term dataset of the CloudSat mission. In this study, we considered the different regions of India to analyze the properties of clouds all through the ISM active and break periods. Using a more extended dataset improves the number of data points selected for a particular region.

The following are the objectives for this paper:

1. To investigate changes in the developing VSC between two ISM spells over selected regions in India.
2. Which predominant clouds are present over these selected regions during different spells of the monsoon?
3. To investigate the microphysical parameters related to the ISM spells and the role of microphysics in precipitation formation.
4. How is the variability in the VSC properties related to the large-scale monsoonal circulation?

The paper is organized as follows: Sect. 2 briefly highlights instruments and the dataset used, emphasizing the methodology adopted. Section 3 discusses the results. Section 4 summarizes the major findings of this work.

2 Data and methodology

Active and break ISM days are identified based on the criteria suggested by Rajeevan et al. (2010) using the Indian Meteorological Department's high-resolution gridded daily rainfall data. Daily rainfall over the ISM core region, central India, is averaged. The result is standardized by subtracting it from the long-term standard, i.e., 1951–2000, and then dividing it by its daily standard deviation. The active (break) ISM periods are defined as the duration for which the above result (standardized rainfall anomaly) is more than +1.0 (less than –1.0), successively for three or more days. Table 1 shows the active and break ISM days for the period 2008–2016 (data is not available for the year 2011). 2012 and 2013 were good monsoon years and hence the frequency of active days was higher compared to break days. The lesser number of break days present in those two years did not fulfill the criteria of standardized rainfall anomaly less than -1.0 successively for three or more days. Therefore, in 2012 and 2013, no CloudSat observations were taken during the break periods. Using the information based on the central Indian active and break ISM days, VSC properties for different places have been studied.

A 94 GHz Cloud Profiling Radar (CPR) on board the CloudSat has resolutions of 1.4 and 1.7 km for cross- and along-track, respectively. It is a part of the A-train

Table 2 Regional 0 and -40 °C height levels during peak ISM (July and August)

Region	0 °C level (km)	-40 °C level (km)
WI	5.3 (± 0.19)	10.8 (± 0.13)
NW	5.1 (± 0.28)	11.5 (± 0.20)
CI	5.6 (± 0.24)	11.4 (± 0.25)
CE	5.2 (± 0.15)	11.3 (± 0.15)
NI	5.7 (± 0.41)	11.8 (± 0.39)
WB	5.5 (± 0.21)	11.5 (± 0.02)
EI	5.1 (± 0.31)	11.6 (± 0.68)
SI	5.0 (± 0.33)	11.1 (± 0.12)

constellation. With its ~ 240 m vertical resolution, CPR can examine optically thick large-particle cloud layers but cannot probe the optically thin clouds, viz., high-altitude cirrus. Further information on CloudSat is documented in Stephens et al. (2008). Gambheer and Bhat (2001) studied the diurnal organization of convection over the ISM region. According to that study, over the landmass of India, local afternoon hours favor the formation of clouds, while the morning hours are least favorable. Moreover, CloudSat passage is more continuous around 1330 LT (day) than 0130 LT (night). Thus, the present study over the ISM region utilizes CloudSat Level 2v05 data sets of the day, 1330 LT, for 2008–2016 to examine the characteristics of VSC over the Indian region.

The discovery of an additional moderate cumulus congestus with shallow and deep convective clouds can be a part of the tropical tri-modal convection (Johnson et al. 1999). Tri-modal convective clouds are a suitable advantage in exploiting the cloud height extent with the cloud vertical structure parameter. Shallow, congestus, and deep convective tropical clouds share the same cloud base height, but their cloud tops exist below 4–5, 7–9, and above 10 km altitude. Sukanya and Kalapureddy (2021) showed the importance of the interaction among the tropical tri-modal convection through the local temperature (especially the 0 and -40 °C height levels) profile-driven three estates within the VSC during the ISM using ground-based cloud radar measurements over the Western Ghats (WGs) of India. They account for the combined vertical structure of cloud and temperature, which is capable of both macro- (micro-) physical classification for three estates of cloud viz., low (warm), mid (mixed), and high (ice) level (phase) cloud with solely the VSC parameter. The present study extends their ground-based VSC to the space-based cloud radar measurements to investigate core monsoon and geographically adjacent regions over India. Table 2 presents the mean 0 and -40 °C height levels during July and August months for the eight regions over India. Das et al. (2011) work on TRMM melting layer height

characteristics over the Indian region is in close agreement with the second column of Table 2.

The following CloudSat datasets have been further utilized in this study.

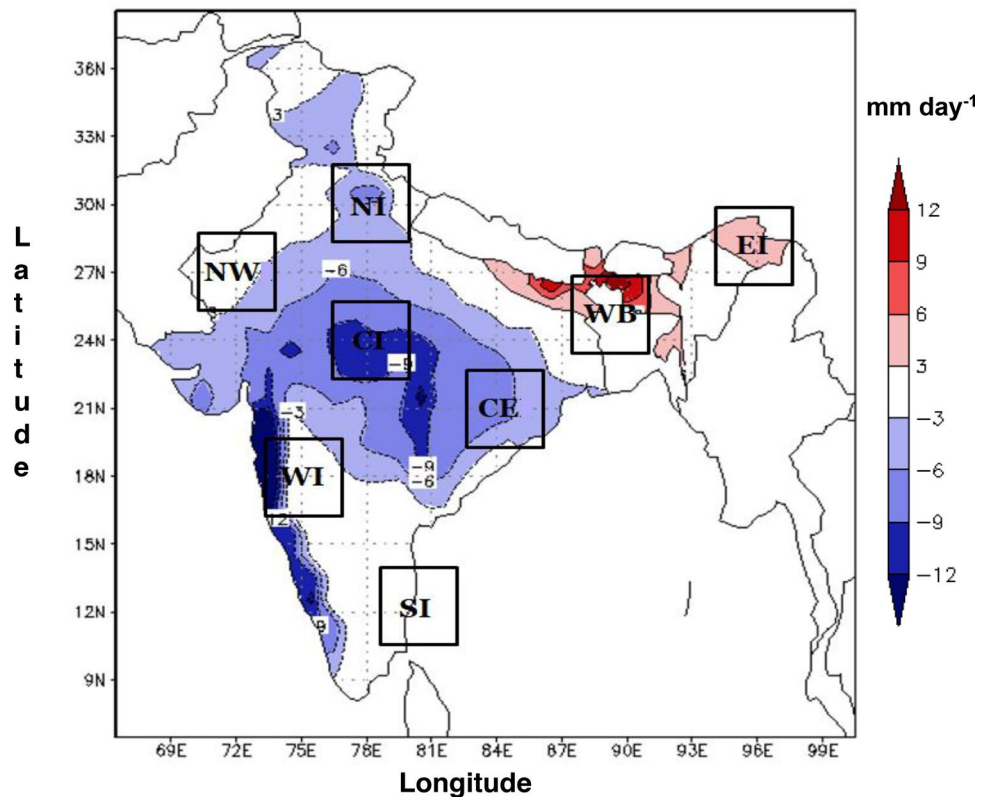
1. 2B-GEOPROF (Radar Reflectivity, CPR cloud mask)
2. 2B-CLDCLASS (Cloud scenario)
3. 2B-CWC ROV (LWC, IWC, Ice effective radius, and ice number concentration)

In brief, separate ice and liquid cloud water content retrieval method in CLOUDSAT uses a forward model which assumes a lognormal size distribution of cloud particles and active and passive remote sensing data together with apriori data to estimate the parameters of the particle size distribution in each bin containing cloud. CPR measurements provide a vertical profile of cloud backscatter; a measured backscatter value and cloud mask (indicate the likelihood that a particular radar bin contains cloud) are obtained from 2B-GEOPROF. Further details on release 4 of the CloudSat 2B-CWC-RO/RVOD Standard Data Products can be seen with Wood (2008) and Austin et al. (2009).

Cloud-mask and radar reflectivity in a vertical column are offered in the 2B-GEOPROF dataset. It is used to identify vertical structures of clouds over different regions of India. The 2B-CLDCLASS dataset was used to classify the clouds present during active and break ISM spells. Based on different rules for hydrometeor vertical scales, the maximum equivalent reflectivity signature of precipitation measured by the CPR and ECMWF predicted temperature profiles and surface topography height (Sassen and Wang 2008), it classifies clouds into either cumulus (Cu, including cumulus congestus), Stratocumulus (Sc), Nimbostratus (Ns), deep convective (cumulonimbus), Altostratus (Ac), Altostratus (As), Stratus (St), or high (cirrus and cirrostratus) clouds. Effective radius, IWC, LWC, and related quantities for each profile measured by CPR are obtained from the 2B-CWC-RO dataset. This retrieval for ice and liquid phases is performed separately. The two sets are then merged to obtain a seamless composite profile with the input measurements (Austin et al. 2009).

For the present VSC analysis, we have taken a representative eight regions over India with $3^\circ \times 3^\circ$ grid boxes that can be seen in Fig. 1. The selected regions are Western India (WI), North-West India (NW), Central India (CI), Central-East India (CE), North India (NI), West Bengal (WB), East India (EI), and South India (SI). These regions are identified based on the progress of the monsoon trough, mainly regions that are influenced by the movement of the CTCZ. WI region consists of some parts of the Western Ghats, which is considered the highest rainfall region in India. We adopted a composite technique to get many data points for each region. Here for active or break composites over $3^\circ \times 3^\circ$ grid resolution, the average number of data points varies for each region from 23,173 to 28,075. Using the equivalent

Fig. 1 Eight different ISM regions selected for this study within $3^\circ \times 3^\circ$ grids, each overlay on rainfall anomaly during ISM break spell on the Indian map



radar reflectivity factor (Z_e), the mean VSC for various locations is examined. Using the cloud scenario variable from the 2B-CLDCLASS product, different clouds are identified, and the frequency of occurrence of different clouds is calculated. In addition, microphysical properties such as LWC, IWC, ice effective radius (IER), and ice number concentration (INC) are investigated from the 2B-CWC RO product.

3 Result and discussion

3.1 Contrasting ISM spells: relative humidity and horizontal wind anomaly

The reason behind the investigation of VSC focussing on the active and break ISM spell is explained in this section. This section brings out the contrast in the background dynamical and thermodynamic conditions during ISM active and break days. Figure 2 shows the composite mean horizontal wind component above the shaded mean relative humidity (RH) for all nine years of active (left panels) and break (right panels) days at four different pressure levels; 1000, 850, 600, and 300 hPa. Strong (weak) low-level moist (dry) westerly jet winds are predominant during active (break) ISM over peninsular India. The conspicuous strong cyclonic circulation over central India at 600 hPa level is the contrasting difference between active and break ISM. The high-level

anti-cyclonic circulation-driven tropical easterly jet feature is omnipresent over peninsular India during both the ISM spells. RH in the two ISM spells mainly differs at mid-level and high-level. Likewise, horizontal wind speed and direction mainly show contrast at 850 hPa onwards. The detailed discussion of using these background conditions for the observed VSC can be found in Sect. 3.5.

3.2 Contrast in VSC during the active and break ISM spells

Contoured frequency by altitude diagram (CFAD; Yuter and Houze 1995) analysis has been chosen for investigating the VSC pertinent to ISM active and break periods. The composited nadir profiles of CloudSat swath data during 2008–2016 have been utilized for constructing the CFAD that explains the statistical distribution of the Z_e . CFAD is a 3-D contour plot of a histogram height profile that summarises normalized histogram analysis of Z_e profiles as a representative cloud vertical structure. It also overcomes the inhomogeneity in space and time scales of radar data. Typical CFADs of Z_e are derived for eight different regions (see Fig. 1) over India for the active and break ISM spells, and composite VSC are shown in Figs. 3a–h and 4a–h, respectively. The NW (EI) shows maximum (minimum) cloud height during ISM active spell. The NW, CI, CE, and WB VSC show cloud heights of more than 16 km, indicating

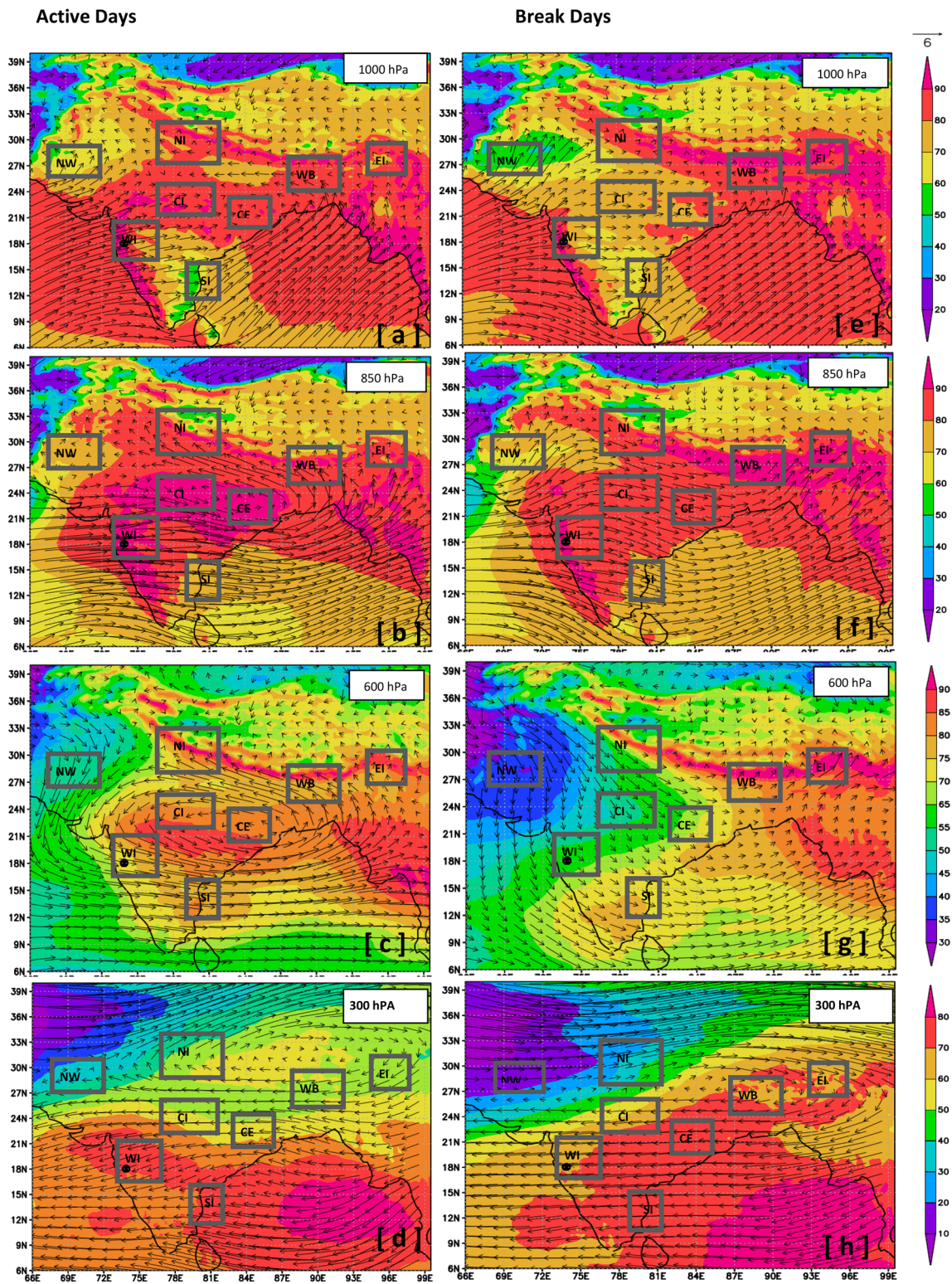


Fig. 2 Shaded RH with horizontal wind imposed on it for (left panel) active (right panel) break days for **a, b** 1000 hPa, **c, d** 850 hPa, **e, f** 600 hPa, **g, h** 300 hPa

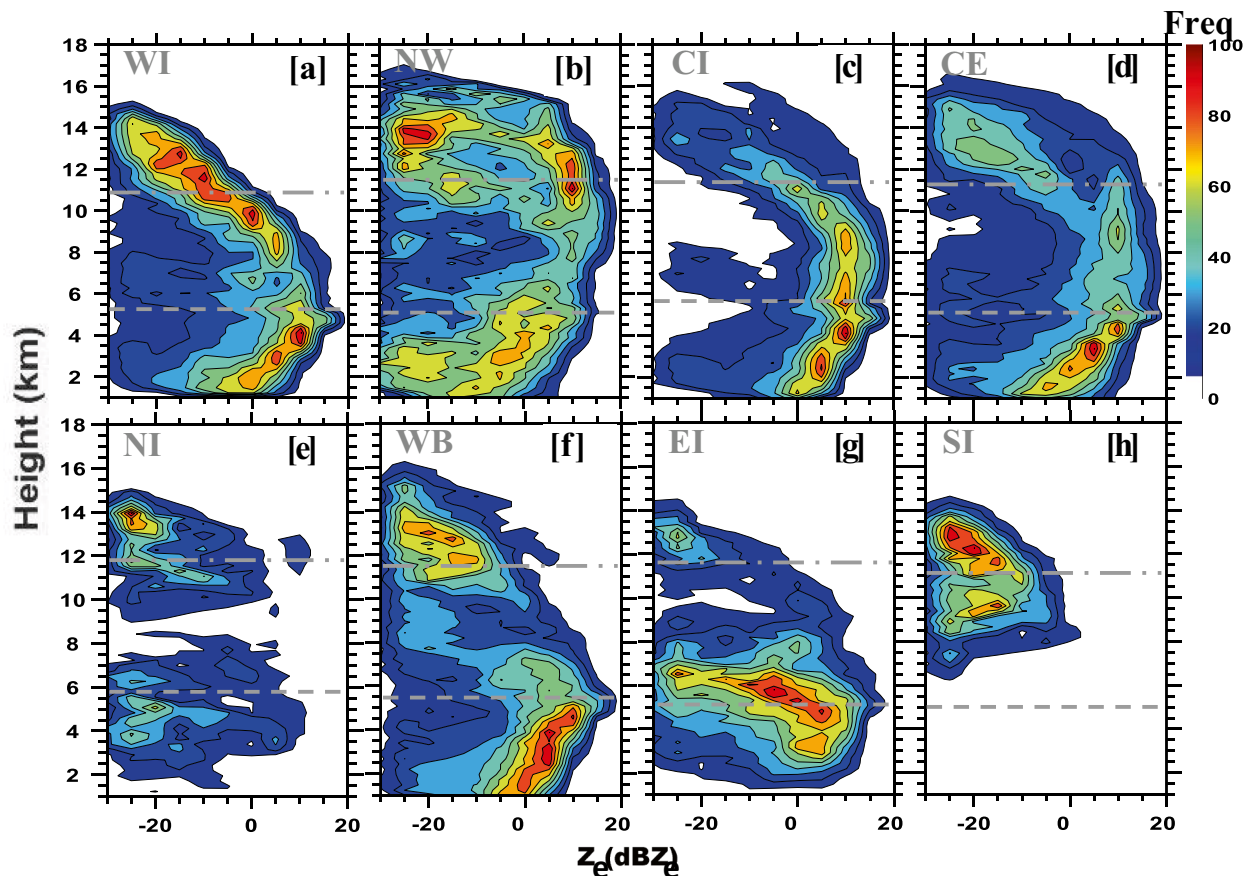


Fig. 3 Contoured frequency by altitude diagram (CFAD) of CPR measured Z_e for **a** WI region, **b** NW region, **c** CI region, **d** CE region, **e** NI region, **f** WB region, **g** EI region, and **h** SI region during ISM active spell

the dominant existence of convective updrafts. The highest VSC over NW shows a wide range of reflectivity, with cloud heights reaching as high as 17 km. Moreover, a peculiar presence of higher frequency above 10 dBZ_e values in the cold cloud region (> 12 km) with the NW VSC infers the predominance of deep convective updrafts owing to monsoon heat low conditions. The influence of low-pressure and cyclonic circulation extends up to mid-tropospheric levels, and monsoon troughs' oscillation over the North causes widespread rain, thundershowers and lightning are likely around Rajasthan (~27° N). However, CE, CI, and WB show a high frequency of above 10 dBZ_e in the cold cloud region but are relatively weaker than NW.

It is interesting to note that VSC over EI show discontinuity due to its location coming under deficit ISM rainfall (break-like condition; see Fig. 1) during the active ISM period. However, EI offers continuous VSC up to 15 km during ISM break periods, whereas NI shows VSC confines only below 8 km infers the predominance of relatively weaker convective updrafts. The VSC discontinuity over NI during active ISM is partly because of the extreme northward march of the monsoon trough limits around the NI

region i.e., 30° N, which results in dry mid-tropospheric condition (see Fig. 2).

The striking difference between active and break ISM is seen over WI, NW, CI, and CE region CFADs. It shows continuous or un-truncated cloud vertical structure during active ISM spell due to the ubiquitous presence of Johnson trimodal convection, thus the interaction among the three-level (warm, mixed, and ice phase) cloud regions/ estates within the VSC. On the other hand, break in the VSC (gap exists in the mid-level mixed-phase) because the clouds are mainly present in either or both warm and ice cloud regions during break ISM days. Space-borne CPR does not detect signals from heavy rain due to the signal attenuation from bigger raindrops. Hence decreasing values of Z_e with decreasing height can be observed below the bright band. Therefore, the Z_{CFAD} , in general, is a curved bow or arc shape especially with a higher frequency count of high Z_e values centered in the mixed phase region between 4 and 11 km for all the regions except NI, EI, and SI (WB) region during the ISM active (break) period. Bow-shaped Z_{CFAD} indicates a favorable condition to have both ice (warm) microphysical growth processes from the top of higher (lower) estates in the VSC

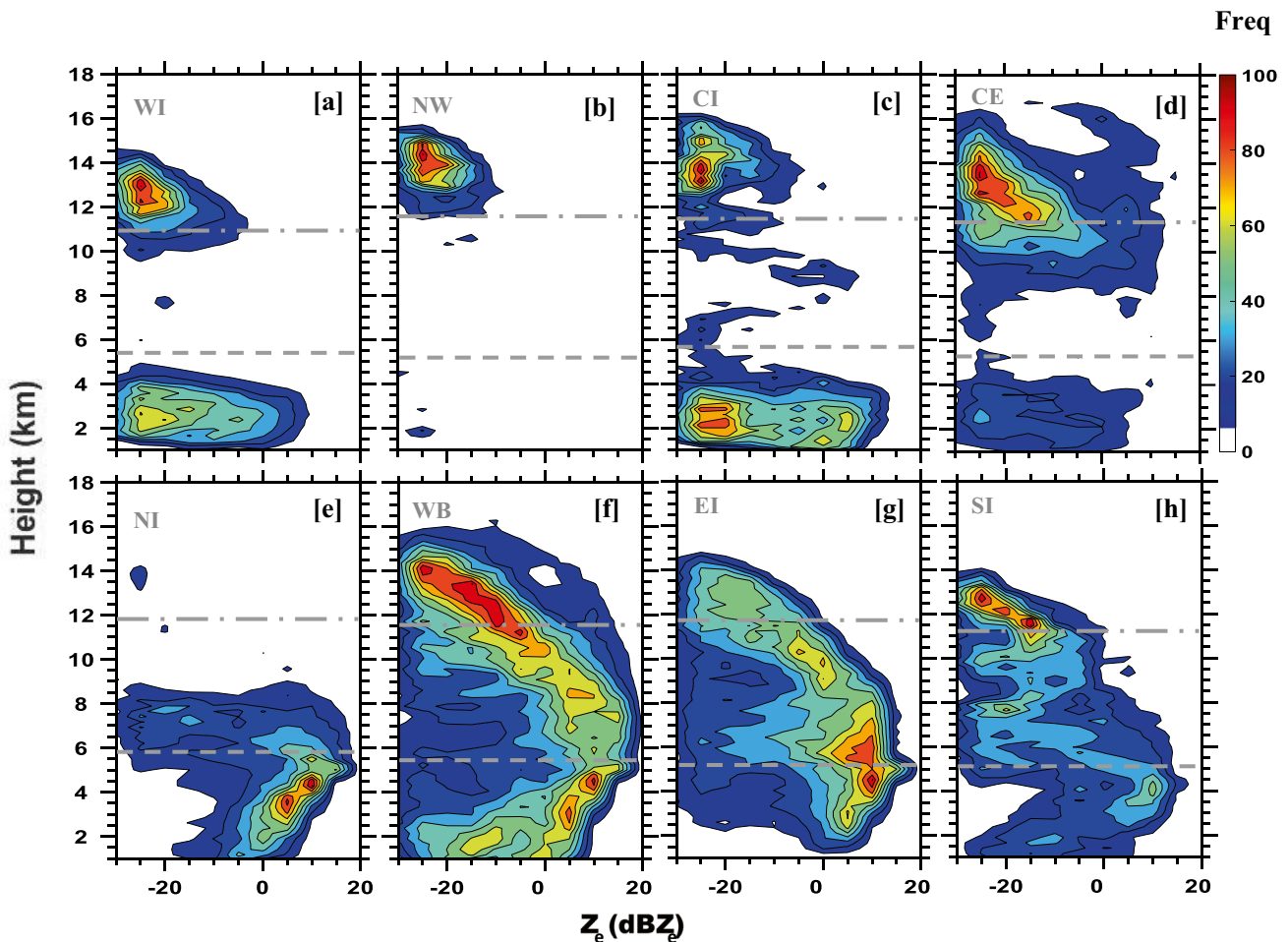


Fig. 4 Same as Fig. 3 but for break ISM spell

(e.g., Figs. 3a–d and 4f–g). In fact, perfect bow shape during active ISM over NW and CE (Fig. 3b, c) indicates deep convective updrafts responsible for the high frequency of Z_e values of above 10 dBZ_e above the -40°C level. Convective precipitation over NW can also be confirmed by the absence of a bright band. Where the VSC is continuous, a bright band feature is observed between 4 and 5 km altitudes, except over NI, NW, and SI, due to the sharp gradient in the value of the hydrometeor dielectric constant at the melting layer resulting in enhanced radar reflectivity. The bow shape is typical to CloudSat's Z_{CFAD} mainly due to the attenuation with CPR (94 GHz) encountering only with lower-level bigger raindrops, below the melting level extending much down to the ground.

Over the WI region, VSC has developed up to 15 km. While higher (lower) values of Z_e , in the range of above 0 dBZ_e with a frequency count more than 50% close to the ground, for active (break) ISM period indicate the formation of precipitating (non-precipitating) clouds in this region. Both on active and break days, the CFAD of WI is similar

to that of CI and CE, which is also indicated by the rainfall anomaly map in Fig. 1. It further indicates a similar mechanism of formation and growth of warm and mixed-phase clouds over these three regions. The exception is at the high level, which shows over WI, more than 60–80% cloud occurrence above 8 km, denoting the predominant ice cloud processes during active days. At the same time, only ~30 (50) % of cloud can exceed 10 km over CI (CE). During the active spell, 50% of the precipitating cloud occurrence is prominent up to 6 km (100% at 2–4 km) in Fig. 3 a, c, and d, with an increase of Z_e values from 0 to 10 dBZ_e. Figure 3a, c, and d also depicts that 40% of cloud occurrence is attributed to ice cloud processes, as the cloud height can touch 12 km from the ground. Secondary non-precipitating cloud patch in the order of -10 to -30 dBZ_e existing at the mid-level (6–8 km) is also commonly associated with the three regions. However, this mid-level mixed-phase cloud is a predominant feature over EI during both ISM spells but peculiar to notice precipitation seldom reaching the ground. Similarly, besides the mid-level weak or cloud void region in

the VSC, above 20% cloud occurrence is mainly limited to up to 5 km at the low-level and 10–16 km at the high-level over WI, CI, and CE during break days. At a low and high level, the maximum cloud frequency concentrated around -25 dBZ_e depicts the dominance of smaller cloud particles or weak layer-type clouds. Besides this maximum frequency, there exists a secondary maximum (50–60%) around 0–5 dBZ_e at a low-level, indicating local precipitation over CI during break ISM. This ground precipitation inferring secondary maximum at low-level clouds can be seen only over CI and WB during break ISM. Predominant high-level clouds during active ISM show extension of its VSC down to the ground during break ISM days, but non-precipitation clouds in nature (above 0 dBZ_e values show frequency count below 30% close to the ground). Over WB and EI regions, during both ISM spells, VSC is continuous and reaches up to 16 and 14 km (Figs. 3f, g and 4f, g), respectively. During the active spell, VSC of WB shows less than 30% of 0 dBZ_e value between 8 and 10 km, whereas a relatively higher frequency of above 5 dBZ_e values between 6 and 10 km indicates intense convection during break ISM days. VSC over EI during break days (Fig. 4 g) is an extension of its active ISM feature of dominant mixed phase supported by higher-level ice microphysical growth. CFAD over the SI region shows high cloud occurrence from 6 to 14 km due to the presence of thick ice clouds or descending cirrus clouds. The absence of low clouds portrays the absence of ISM rain over this region. Since the high-level clouds lag with respect to the convection center (here it's CI) during active days (Jiang et al. 2011), it explains the presence of predominant high clouds and the complete absence of low or mid clouds over the SI region. Though, VSC over the SI region is continuous during break days having a weaker frequency count of $\sim 30\%$ at a lower-level resulting in the absence of ISM rain over this region.

Over the NI region, in both the ISM spells, low-level cloud top exists ~ 8 km with a weaker 30% cloud occurrence above the melting layer. Further, active days are dominated by non-precipitating clouds (below -20 dBZ_e). It is observed that the most significant contrast between active and break ISM spells is observed over all regions except WB and EI regions (Figs. 3f, g and 4f, g).

3.3 Occurrence frequency of warm, mixed, and ice phase clouds during the ISM active and break days

This section offers the study of the occurrence frequency of clouds inside the three different cloud zones depending on the phase of the cloud particles, namely warm or low (below 0° isotherm), mixed or mid (0 to -40 °C), and ice or high (< -40 °C) cloud region. Histogram analysis of CPR measured Z_e normalized with the maximum occurrence value

serves the purpose as shown in Fig. 5. As revealed in the previous section, along with the structure of the cloud, further contrast can be seen in their number of occurrences during the two ISM spells. Over WI and NI, the distributions of cloud at the low and high levels are negatively (positively) skewed during active (break) days indicating the dominance of higher (lesser) Z_e. Interestingly over WI, cloud presence at the mid-level is two times higher in the active spell than in the break spell. During break days NW region shows maximum cloud occurrence below 20% except at the higher level. A meagre difference in cloud frequency is observed over CI and CE regions at mid and low levels from small to medium-sized cloud drops (-50 to -5 dBZ_e) in active and break spells. Big cloud drops or large number of small cloud drops of Z_e > 0 dBZ_e are significantly dominant at the low and mid-level during active days. In contrast, maximum frequency at -35 dBZ_e during break days dictates the predominance of weak high-level clouds. Bimodal distributions at low-level are salient features for both WB and EI regions, revealing the presence of rainy and non-rainy cloud types. Almost similar frequency of cloud over WI and EI during active and break spells leads to a similar type of VSC in the two ISM spells found in the previous section. Unlike CI, a higher value of Z_e (> 5 dBZ_e) is more dominant during the break spell. EI region consists of high Z_e value (< 10 dBZ_e) at low levels and higher ($> 60\%$) occurrence of cloud in both the spells at all the levels, which is in contrast to other regions. All regions show that high-level cloud occurrence is maximum compared to the other two levels, irrespective of the monsoon spells. Due to the unfavorable large-scale condition, the SI region is deprived of the low-level cloud occurrence during active days and the maximum Z_e value is limited to 5 dBZ_e, unlike other regions. One must not ignore the lesser Z_e value at low levels compared to mid-levels over most regions which restricts our study from comparing the two levels over the same region. It might occur due to the attenuation from the rainy cloud of the small wavelength of CPR observed from space.

3.4 Latitudinal variation of VSC during the ISM active and break spells

The contrast of composited cloud vertical structure with different latitudes during active and break days for 2008–2016 is shown in Figs. 6 and 7, respectively. Besides the present study regions, a 3° x 3° box around the equator (EQ) is also included in this section to understand the northward propagation of the cloud belt from the equator. During Active days due to the northward propagation of the cloud belt towards the CI region, CI, CE, WI, and WB regions show complete VSC due to the frequent occurrence of deep convective clouds. On the contrary, EQ SI regions show the dominance of either low cloud or high cloud with the isolated

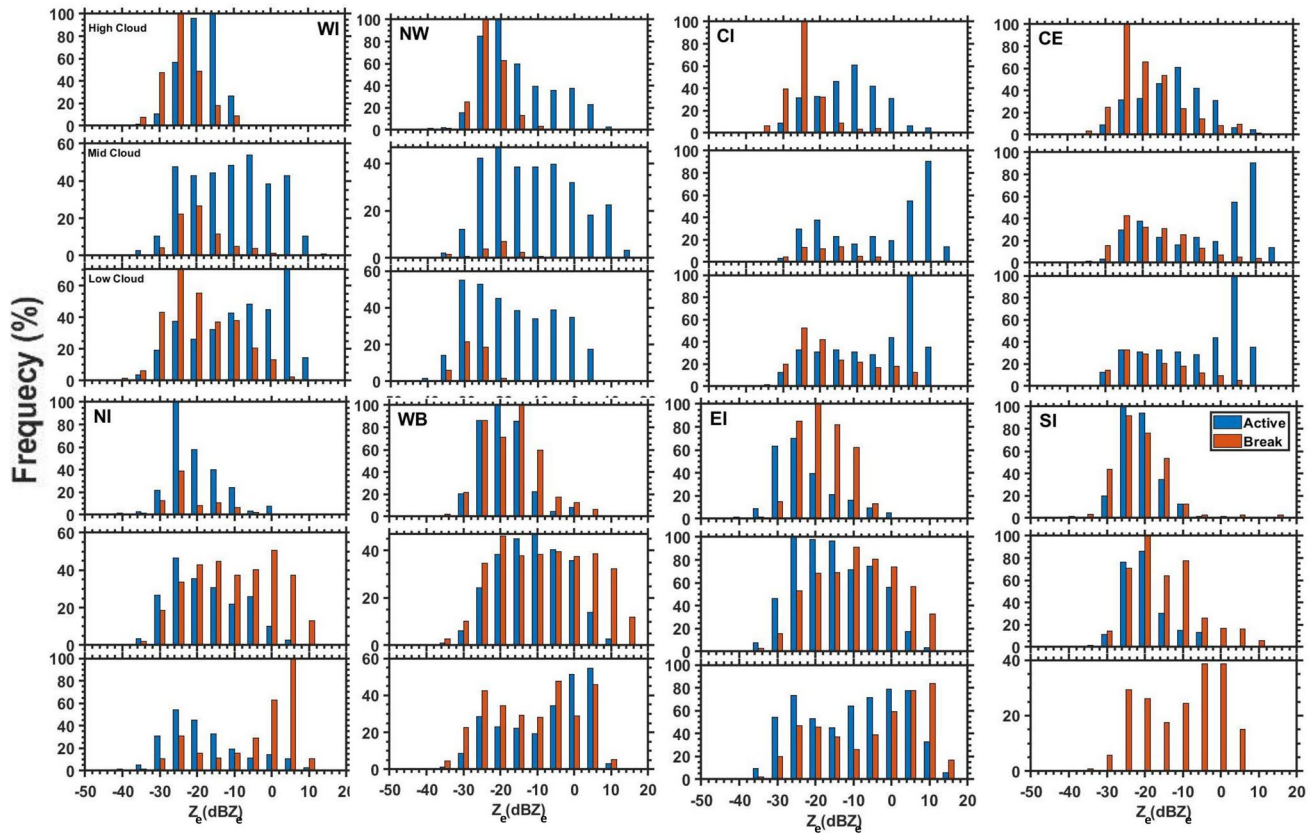


Fig. 5 Histogram analysis of CPR measured Z_e for **a** WI region, **b** NW region, **c** CI region, **d** CE region, **e** NI region, **f** WB region, **g** EI region, and **h** SI region during ISM active (blue bar) and break (red bar) spell

presence of deep cloud towards the north of the EQ. Few cloud occurrence over NI shows the dominance of warm clouds. Over the EI region, after 28° latitude, cloud height decreases as the dominance of mid-level clouds and high clouds increases. Due to the few cases of deep clouds over the NW region, some of the latitudes show a void of cloud in the whole VSC. Maximum Z_e of 20 dBZ_e reaches above 10 km over CI compared to other deep convective cloud regions. During break days, cloud occurrence decreases severely over CI and NW, showing the occurrence of only warm clouds or multi-layered clouds and cirrus clouds reduced to the presence of only cirrus over NW. A sustained shallow warm cloud with the high-level cirrus cloud over the WI region leads to the broken VSC. The maximum Z_e over those regions is reduced to 10 dBZ_e or below than active days. In contrast, a complete VSC region can be found over EQ and EI due to the incessant presence of deep clouds along the latitudes, in contrast to the active day's VSC. The deep cloud is persistent over WB, similar to active days. However, during break days, the maximum Z_e of 20 dBZ_e is limited to certain latitudes. CE and SI regions show the mixed occurrence of shallow and deep convective clouds. Mid-level congestus are predominant in the NI region.

3.5 Background condition behind the formation of VSC

To investigate the background condition of these contrasting VSC, horizontal wind is plotted above the shaded relative humidity (RH) at the left and right panels in Fig. 2 for active and break days, respectively. Southwesterly wind is more intense at the surface during active days than break days as shown in Fig. 2a, e especially from central to south India. During active ISM, relative moisture deficiency over the SI region in the low levels (Fig. 2a) is responsible for the missing warm cloud of SI in Fig. 3h. During break ISM, the mid-tropospheric levels (600 hPa) over WI, CI, and CE regions show relatively deficit RH values and much drier (below 40%) over the NW region. Moreover, the CE and SI region shows improved RH values at 300 hPa level. This high-level adjective moistening may be due to the TEJ from the anticyclonic circulation. During break ISM, relatively higher moistening is seen at 300 hPa level over CE, SI, and WB regions, which is conducive to maintaining the higher frequency count of cold clouds seen in CFADs of Fig. 4d, h, f, respectively. The gradual reduction of RH from the surface to the upper level is prominent during break days

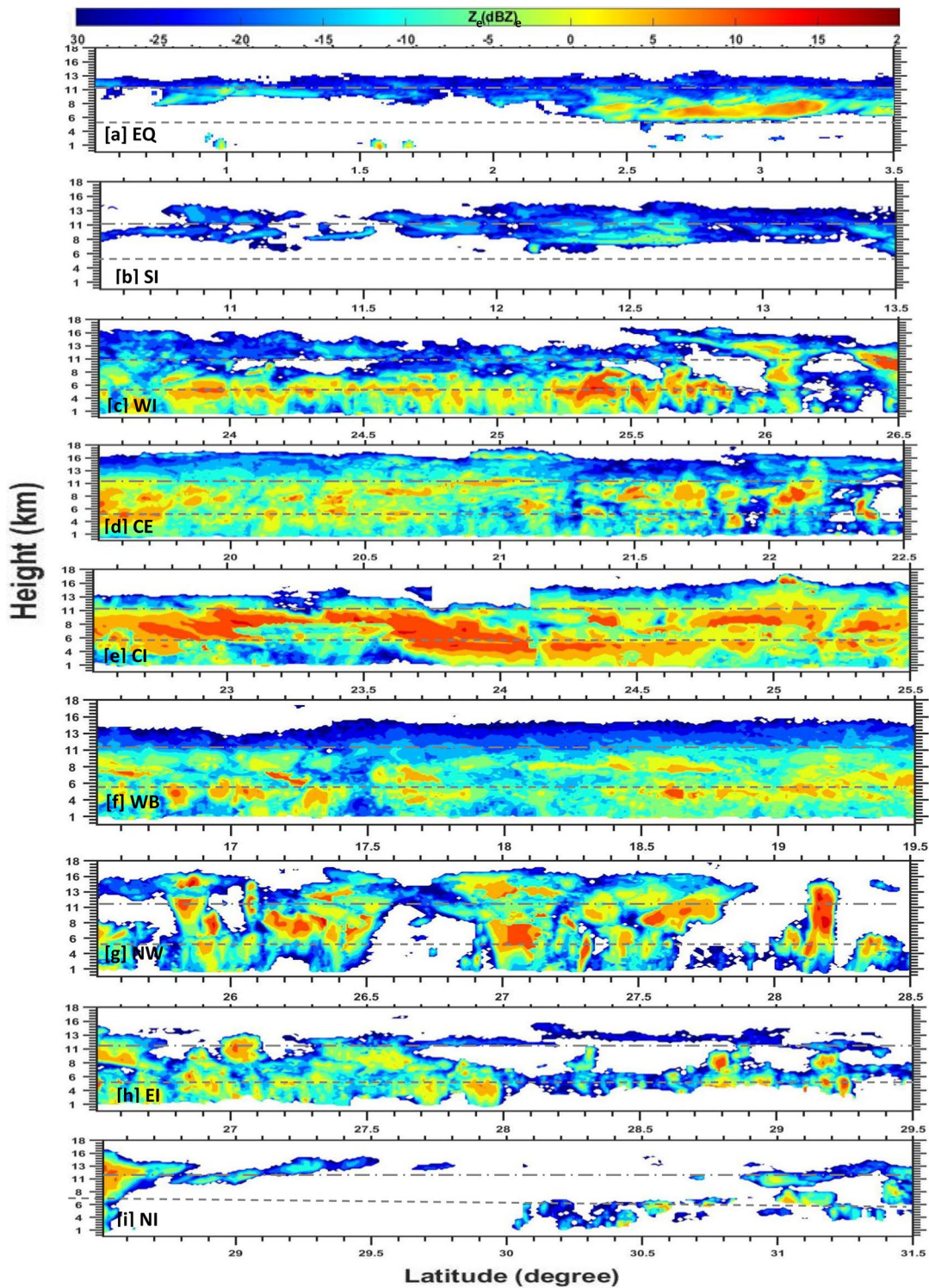


Fig. 6 Latitudinal variation of VSC over a EQ, b SI, c EI, d WB, e NI, f CE, g CI, h NW, i WI during active days

in Fig. 2e–h. RH also carries the contrast between the two spells since it is 10% lesser than CI and WI during break days. The cyclonic circulation generated over the head of the Bay of Bengal and above is prominent at 850, and 750

hPa (Fig. 2b–c) is completely missing on break days. Certainly, this cyclonic circulation is one of the important factors in active days to provide ample moisture, especially at the mid-level required for the generation and sustenance

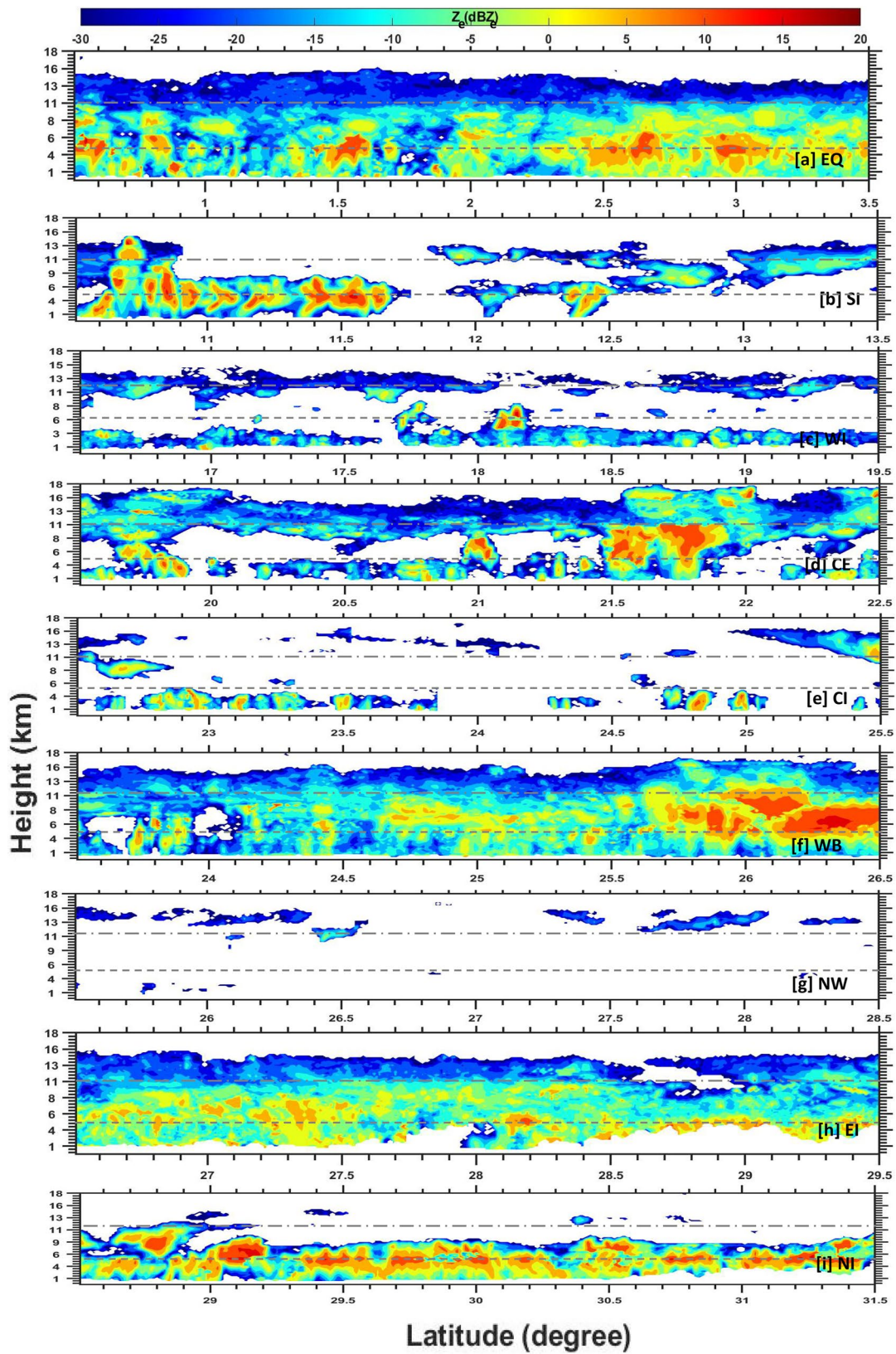


Fig. 7 Same as Fig. 6 but for break days

of deep clouds. The active (break) condition is generally associated with an increase (decrease) of cyclonic vorticity and decrease (increase) of surface pressure over the central Indian monsoon trough region and a strengthening (weakening) of the low-level jet. In Fig. 2g, h, RH at 750 and 550 hPA below 70% over most of the CI and WI region indicate the lack of moisture during break days, limiting the growth of clouds.

During the active period of ISM, the mid-tropospheric vorticity over the northern Arabian Sea (AS) and northern BoB experience anomalous intensification. Due to synoptic-scale cyclonic anomalies at midlevel, the West coastal zones of India favor medium systems. At the same time, BoB and Myanmar's west coast are favorable for larger systems to develop. Enhanced stratiform precipitation areas and new convection are triggered due to southwesterly low- to mid-level flow, which is advected directly across the mountainous coastlines (Medina et al. 2010). Zuidema (2003) proposed that deep convection over the BoB could be initiated by the land–water interface, is important for the convection genesis and thereby affects the spatial distribution of convection. At the same time, the thermodynamic and dynamic structure in the mid-troposphere can trigger deep convection in a conditionally unstable situation.

During the ISM active period, the NW region receives rainfall from the abrupt, intense convective systems formed due to the formation of lower tropospheric heat low over Pakistan and the adjacent region (Sikka 1978; Hunt and Fletcher 2019). The most efficient ISM rain-producing system is known as the synoptic scale disturbances, viz., monsoon low-pressure areas and monsoon depression (MD; e.g., Sikka 1978; Hunt and Fletcher 2019). The MD propagates deeply into the continent and produces large amounts of rainfall systems along its track, and about half of the monsoon rainfall is contributed by the MDs (e.g., Hunt and Fletcher 2019). MDs form over the BoB warm surface within the moist environment of monsoon air and move in the west or northwest direction along the monsoon trough towards the warmer and drier environment of the heat low system over western India and Pakistan (Sikka 1978). This low-pressure system draws surface moisture from the BoB branch of ISM by eastward-moving low-level jet (LLJ). During the break time, LLJ direction is changed to southeastward. There is no LLJ through peninsular India (Joseph and Sijikumar 2004), resulting in a deficit of moisture transport over this region. Also, due to the arid conditions of this region, moisture drawn from offshore is dried out due to prevailing dry conditions. It results in the drying of the mid and lower troposphere.

It is observed that during the ISM active spell, CI and CE regions are under the influence of synoptic systems. These synoptic systems form over the BoB and move

NorthWestward along the trough line (Rao 1976; Mooley and Shukla 1989; Goswami et al. 2003). These synoptic-scale disturbances intensify the low-level southwesterly jet and withdraw moisture from BoB. It impacts precipitation and the vertical development of clouds. Mainly, adverse impact is observed over the CI and CE region during the different spells of monsoon. The VSC observed over CE, and CI is similar to each other both in the active and break spell. However, the occurrence frequency of lower reflectivity indicates the presence of thin, non-precipitating clouds.

Small systems form over the western foothills of the Himalayas because of low-level moist air, which is also associated with instability. This low-level moist air is capped by dry westerly flow aloft and then is lifted over the foothills (Medina et al. 2010).

During the active spell of ISM, precipitating clouds are formed over WB due to the convergence of moist monsoonal air with Himalayan elevations driven by daytime heating over the Tibetan Plateau (Houze et al. 2007). During the break period, monsoonal wind patterns over this region are normal to the orography leading to enhanced deep convection over this region and the concave indentation of Himalayan orography.

Over EI, distinct rainfall patterns were observed due to low-level zonal wind fluctuations and their interaction with regional-scale topography (Fujinami et al. 2014). Over this region, broad stratiform cloud systems are formed as a part of Mesoscale convective systems in association with BoB depressions (Houze et al. 2007). Monsoon depressions formed near Head BOB and propagat into the Indian region through monsoon trough over Indo-Gangetic Plain and make a substantial amount of rainfall over EI. Monsoon depressions provide a moist maritime environment favorable for convection, allowing the mesoscale systems to develop larger stratiform clouds. SI shows similarity in the VSC for both the ISM spells but layered clouds in higher levels are seen during the break period (Figs. 3h, 4h). VSC properties over WB and EI are observed fairly consistently during the active and break spells. Due to the weakening of descending flow in the mid-troposphere from the Tibetan Plateau generated by mechanical and thermal effects during ISM months which helps deep convection to develop (Sato and Kimura 2007). SI region comes under the rain shadow region during ISM. SI receives rainfall from the northeast or retreating monsoon from October to December (Rao 1976).

3.6 Occurrence of different types of clouds

Figure 8 shows the normalized cloud type frequency over the selected Indian regions derived using the CloudSat 2B-CLDCLASS product. St and Sc clouds are not well separated in the 2B-CLDCLASS product and hence

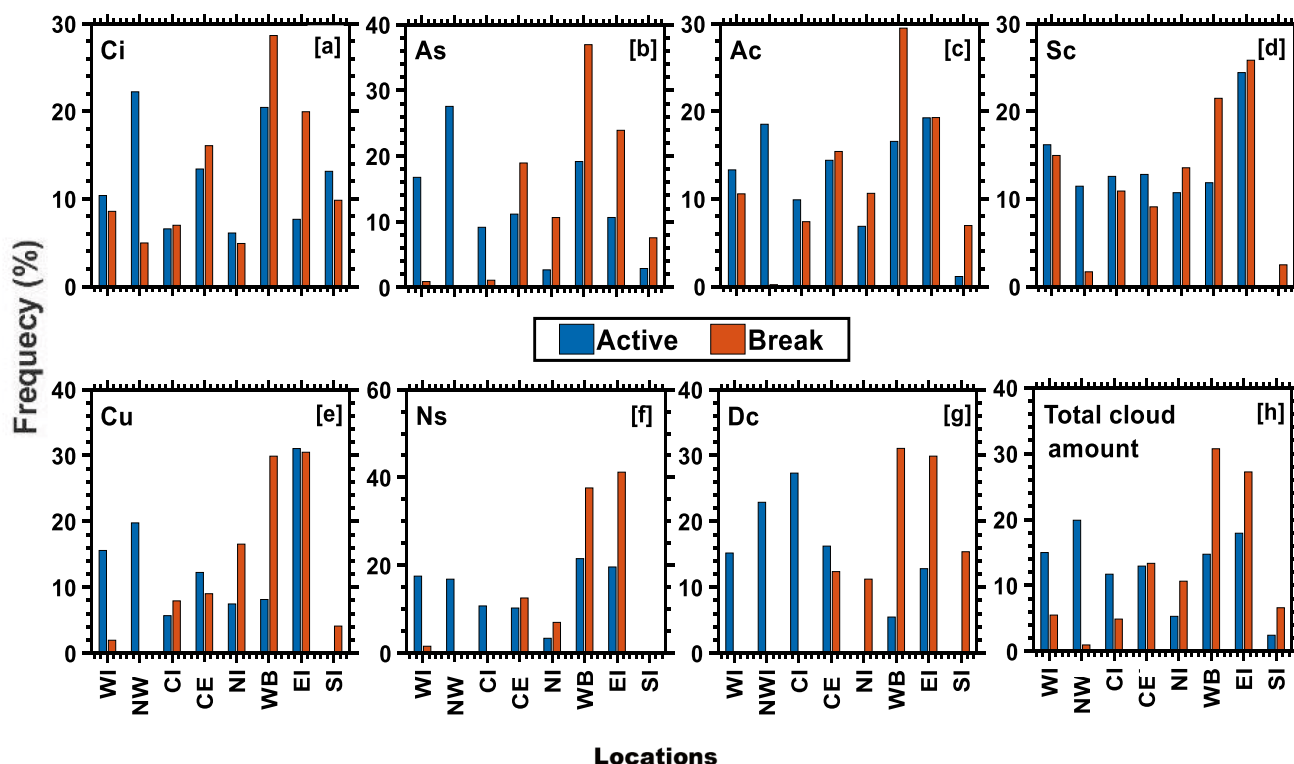


Fig. 8 Different types of clouds **a** Ci, **b** As, **c** Ac, **d** Sc, **e** Cu, **f** Ns, **g** Dc and **h** total cloud amount present in percentage during ISM active and break spells over different regions of India

combined for further analysis. It is also documented that over the Indian region occurrence of St and Ns Cloud is nominal (Subrahmanyam and Kumar 2013). Figure 8 h shows that during both spells of monsoon, mainly three types of clouds at the mid-level (Ac and As) and high-level (Ci), are showing a higher percentage of occurrences. It is observed that As clouds are dominant during the active period. Previous studies of cloud types over the Indian region suggested the presence of Ac cloud over Indian landmass during ISM months (Subrahmanyam and Kumar 2013). Unlike many boundary layer clouds, mid-level clouds cannot be maintained by surface moisture fluxes. Hence, the presence of mid-level clouds over the Indian subcontinent indicates the presence of large-scale convection.

In Fig. 8a, it is observed that Ci clouds are present most prominently over the NW (WB, CE, and EI) region during the active (break) ISM period. During the ISM, monsoon depressions are formed in head BoB resulting in the formation of Ci clouds (from anvils of deep towers). Higher-level strong Tropical Easterly Jet (TEJ) spread these clouds over the ISM region (Sathiyamoorthy et al. 2004). It is to be noted that Ci cloud occurrence is underestimated by CloudSat since it is not sensitive to optically thin clouds.

Figure 8b and c show As and Ac cloud's distribution over all selected Indian regions. It is seen that Ac and As

clouds most frequently occur over CE, WB, and EI regions. As discussed above, VSC over these regions is under the influence of monsoon depressions and is favorable for the formation of mid-level clouds. It is also observed that during the active (break) period, As and Ac clouds show higher occurrence frequency over NW (WB) regions. The relative occurrence of Ci, As, and Ac follow similar distribution over WI, NW, CI, CE, NI, and WB during active days and over WB, EI, and SI during break days. It indicates the proportionate relationship between mid-level and high-level clouds.

Sc cloud is a drizzling cloud that shows a near similar appearance in both the monsoon spells but has a slight increase in appearance during the active period (Fig. 8d). Unlike other cloud types, Sc occurrence is more than 10% in all the regions except for SI and NW, especially during active days. Sc clouds frequency is higher over EI during both the ISM spells (except NW). Cu cloud frequency is reduced for the WI region during the break period. This reduction of the frequency of Cu clouds and the presence of Sc clouds over WI is associated with descending motion of monsoonal convection and intense dry air mixing from Western Asia at $\sim 650 - 500$ hPa (Krishnamurti et al. 2010). This inhibits the vertical development of clouds over this

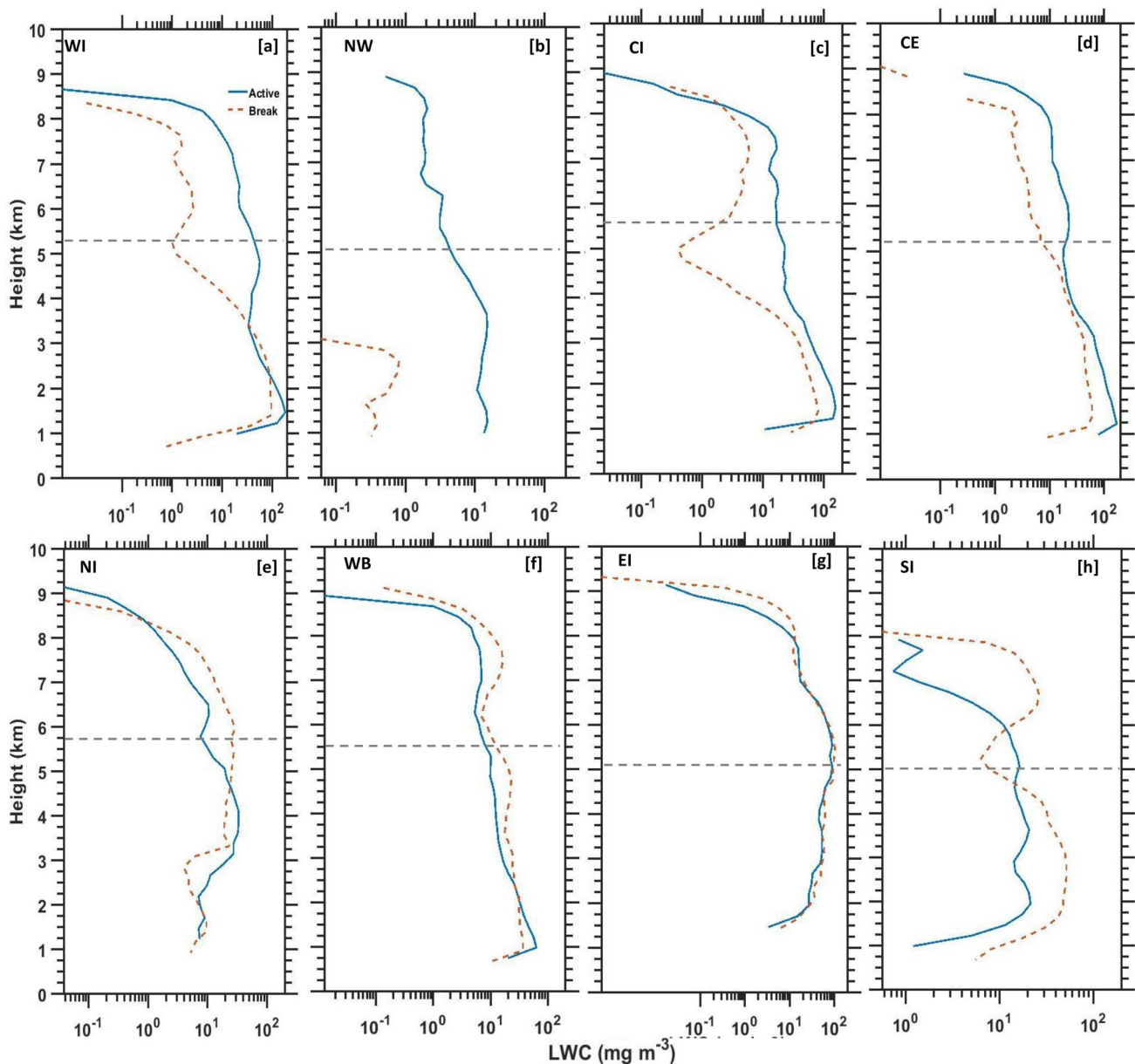


Fig. 9 Vertical profiles of LWC observed over **a** WI, **b** NW, **c** CI, **d** CE, **e** NI, **f** WB, **g** EI, and **h** SI region during ISM active (Solid blue) and break (break red) spell

region. Sc and Cu clouds are more favorable over WB (during break) and over EI (during both ISM spells).

Rain-bearing Ns clouds (Fig. 8f) are present over all the regions during the active spell of the monsoon. These clouds are present over WB and EI during the break period, with maximum frequency observed over the EI region. Over the SI region, Ns clouds are absent during both spells of the monsoon. Dc clouds (Fig. 8g) are present with a higher percentage over CI (WB and EI) during the active (break) period. Earlier studies (Zuidema 2003; Subrahmanyam and Kumar 2013) documented a high presence of Dc over the BoB region. Seesaw in the occurrence of Dc, Ns, and

As clouds (Fig. 8g) is predominantly seen over southwest regions: WI, CI, and NW (Foothills of Himalaya regions: WB and EI) of monsoon trough line in the active (break) ISM spell. It indicates the movement of the monsoon trough, which leads to a change in cloud occurrence pattern and hence, results in rainfall pattern.

3.7 Vertical profiles of LWC and IWC

The vertical profiles of LWC and IWC over the eight regions are displayed in Figs. 9 and 10, respectively. Profiles with the bad flags in 2B-Geoprov and 2B-CLDCLASS datasets

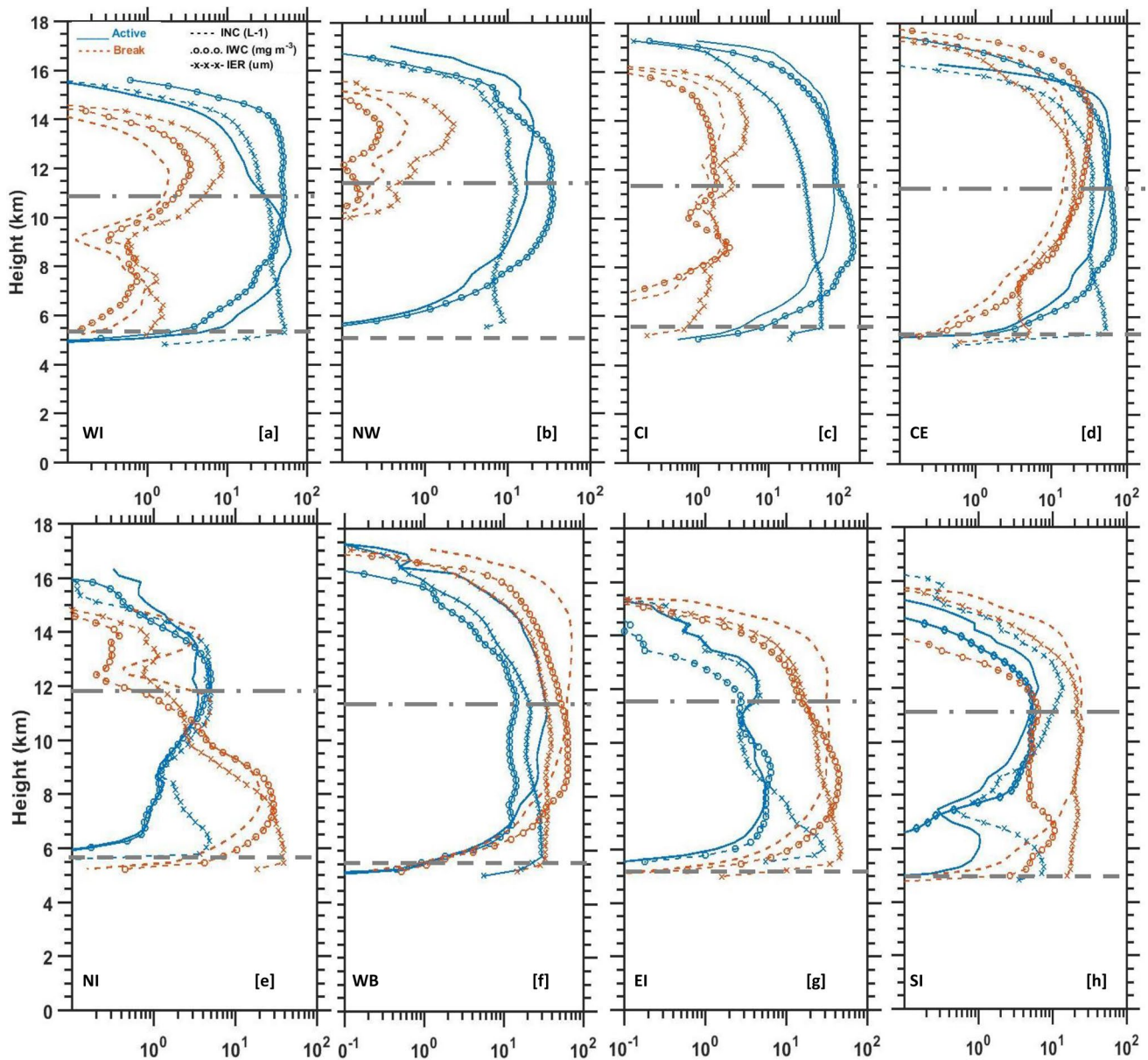


Fig. 10 Same as Fig. 9, but for IWC (circle lines), INC (without marker lines), and IER (crossed lines)

are excluded as these may impact the calculation of LWC. It is observed that during the active (break) ISM period, LWC profiles show a unimodal (bimodal) distribution with peaks at 1.5 km (above 5 km). WI region (Fig. 9a) shows a maximum value of LWC (185 mg m^{-3}) at 2 km altitude during the active period, while the minimum LWC is observed over the NW region ($< 1 \text{ mg m}^{-3}$ Fig. 9b) during break spells. Additionally, the NW region possesses the minimum LWC compared to other places in both spells. CI and CE regions (Fig. 9c, d) shows a prominent contrasting feature with higher LWC during the active period and lower LWC during the break period. Fairly similar values of LWC during both the spells are observed over WB and EI regions

(Fig. 9f, g). EI region shows increased LWC at 5 km for both spells of monsoon. It is to be noted that CloudSat measures profiles from the sea surface. Over Himalayan ranges, the mean surface height is ~ 3 km. Hence LWC Profiles calculated over the Himalayan foothills regions show the effect of orography.

The IWC exhibits unimodal distribution with skewness at an altitude of ~ 9 km during active days. During the break period, skewness is observed towards higher altitudes (> 9 km). It indicates higher ice sedimentation during active spells than during break spells. Core monsoon regions and NWI show one order high values of IWC during the active period than the during break period.

The structure of IWC profiles during both the ISM spells similarized to the ground-based cloud radar estimation over WGs by Sukanya and Kalapureddy (2019) but the difference in spatial resolution of the two radars causes the difference in IWC values. CI (Fig. 10c) and WB (Fig. 10f) regions show the highest values of IWC (160 (65) mg m^{-3}) during the active (break) period. Maximum IWC is observed at ~ 9 km over CI (Fig. 10c) and CE (Fig. 10d) during the active period and over WB (Fig. 10f) and EI (Fig. 10g) during the break period. Webster et al. (1986) showed that monsoon trough shifts towards the foothills of the Himalayas during the break period leading to stronger updrafts over these regions resulting in higher IWC.

3.8 Vertical profiles of IER and INC

The vertical profiles of IER and INC over the eight regions are illustrated in Fig. 10 by dotted and cross-marked lines, respectively. The highest value of IER is observed over CI ($58 \mu\text{m}$, Fig. 10c) during the active period, while over EI ($48 \mu\text{m}$, Fig. 10g) during break period. A peak in IER values is observed at 5–6 km during the active period and 12 km during the break period over all the regions except NI, EI, and SI. Unlike other regions, ten times and 1.5 times higher IER can be seen over NI and EI, respectively, during the break spell than in the active spell. The exact opposite structure of IER maxima can be seen over SI, having a peak of IER at 5 km during the break spell and 10–12 km during the active spell. The most prominent contrast of IER is evident over WI, CI, and CE, having ten times higher IER during active days, indicating dominating ice process than on break days. A higher percentage of cirrus clouds may lead to a secondary peak in IER at 12 km, especially for the regions experiencing a break period. During the active (break) period, it is observed that larger ice hydrometeors with IER greater than $24 \mu\text{m}$ are observed over CI, WI, CE, WB, and EI (EI, NI, and WB) at an altitude of 5–6 km.

INC profiles show that number concentrations increased with height for both spells and were observed to be highest in upper levels. A higher value of INC is observed over CI (90 L^{-1} , Fig. 10c) and WB (48 L^{-1} , Fig. 10f) during the active period and the break period, respectively. The most gradual increase is observed over the regions affected by the monsoon trough, i.e., CI and CE (WB and EI) during the active (break) ISM spell. Hence, the presence of synoptic disturbances over the region might lead to lifting these hydrometeors higher in altitude.

From Fig. 10, it can be concluded that large (small) sized hydrometeors are present in lower (higher) heights with lower (highest) concentrations. Using the CloudSat satellite and ground observation data, Deng et al. (2014) concluded that IER has the best correlation with precipitation at 5–6 km level. This correlation decreases with an increase

in height above 5 km. Aircraft observations show a higher number concentration of ice particles, the existence of small and large cloud droplets, graupel, columns, and rimed needles within the temperature range of -8 to -3 °C. This indicates that the increase in the ice concentration is due to the Hallett-Mossop (HM) process of secondary ice formation (Patade et al., 2016). INC reaching above 5 L^{-1} is representative of the efficient production of ice hydrometeors by ice processes.

Further, it is also concluded that the HM process is responsible for graupel formation. During the active (break) ISM period, IER over the regions CI, WI, CE, WB, and EI (EI, NI, and WB) cross the threshold (5 L^{-1}) for the HM process to start ice production. It suggests favorable conditions for HM in mixed-phase clouds. It also underlines the importance of the role of mixed and ice phase microphysics in ISM.

3.9 Day and Night aspects of VSC

CPR data during 2006–2010 helped us to bring the apparent diurnal aspects by constructing CFAD for the day (1330 LT) and night (0130 LT) passages of CloudSat and also pertinent to Active and Break ISM days in Fig. 11. In Fig. 11, dominant high-level ice cloud reflectivities centered ~ -24 dBZ_e above 12 km altitude show a quick descending growth rate of $\sim 6 \text{ dBZ}_e \text{ km}^{-1}$, which is predominantly seen during local night in Fig. 11b. The relatively less contribution of mid-level mixed phase region, but wide dBZ_e distribution at the warm phase region during the day (1330 LT) as shown in Fig. 11c and d is due to the presence of low-level clouds. These low-level clouds are mainly of precipitating (non-precipitating peak at $\sim -26 \text{ dBZ}_e$) type with a maximum at 0 dBZ_e during active (break) ISM periods. Further, the daytime (1330 LT) local moist convection contribution to the low-level clouds is of the predominant precipitating category during the active ISM days. This local convection is expected to be absent during the night (0130 LT) that has been conspicuously seen during break ISM days. Figure 12a and b represent the mean and standard deviation of RH for active and break days of 2006–2010 from IMDAA 3-hourly data over Mandhardev, WGs. It is interesting to note nocturnal boundary layer height region (~ 1 mm) during moderate to heavy rainfall.

Further, to inspect the difference in VSC between CloudSat and an instrument having a finer diurnal variation of clouds, we utilized IITM's ground-based Ka-band radar (KaSPR) data over Indian Western Ghats (WGs). Zenith looking continuous high-resolution measurements from KaSPR help to explore active and break days of 2014 over Mandhardev, WGs. Figure 13 is the 3-hourly composite CFAD of KaSPR's Ze at every 3 hours. Figure 13a shows that during active ISM days, the cloud occurrence at each

Fig. 11 CFAD of CloudSat CPR's Z_e **a, b** for 13:30 and 01:30 LT, respectively. **c, d** same as **a, b** but for active and **e, f** break ISM (Jul and Aug) days of 2006–2010

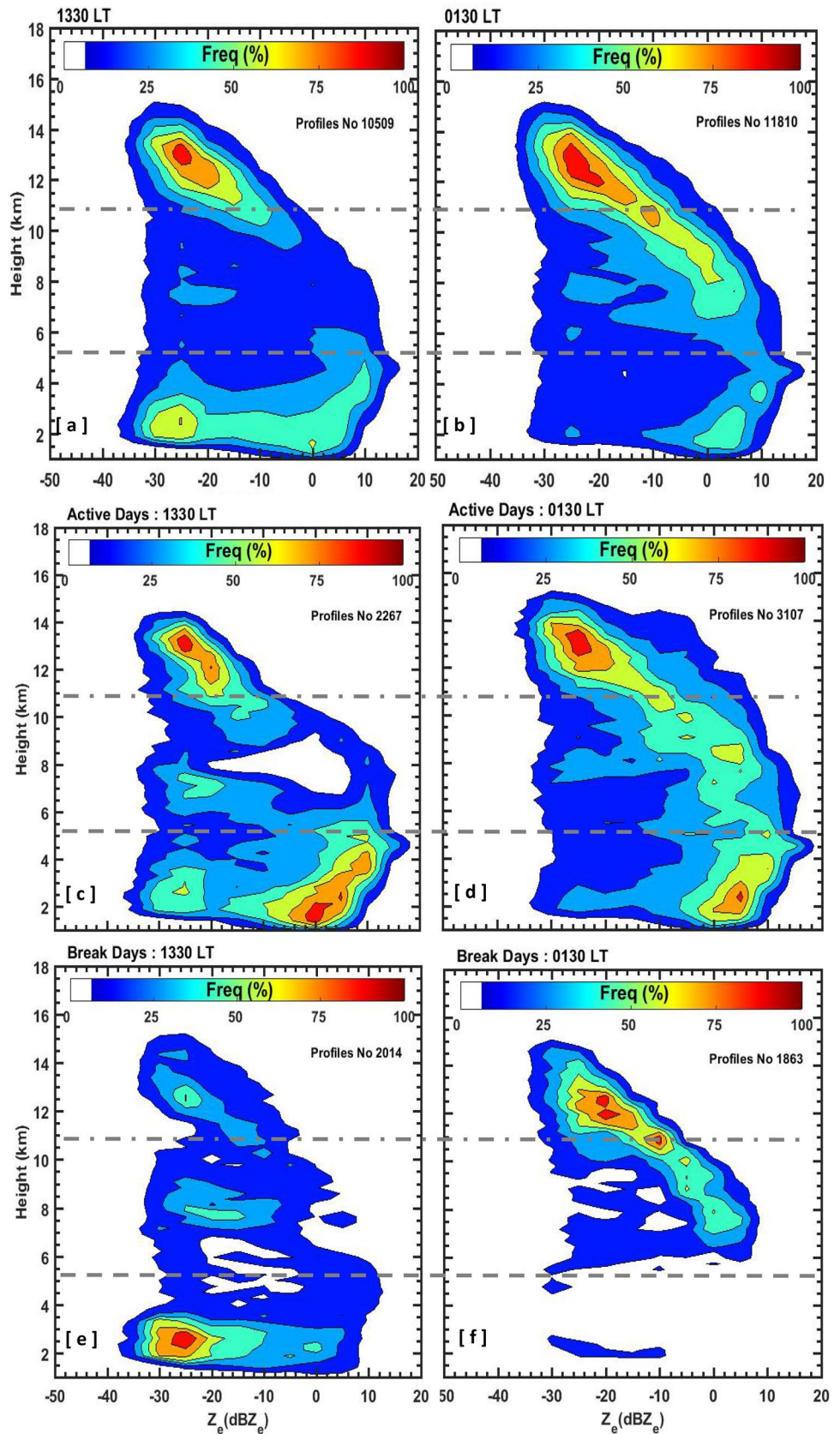
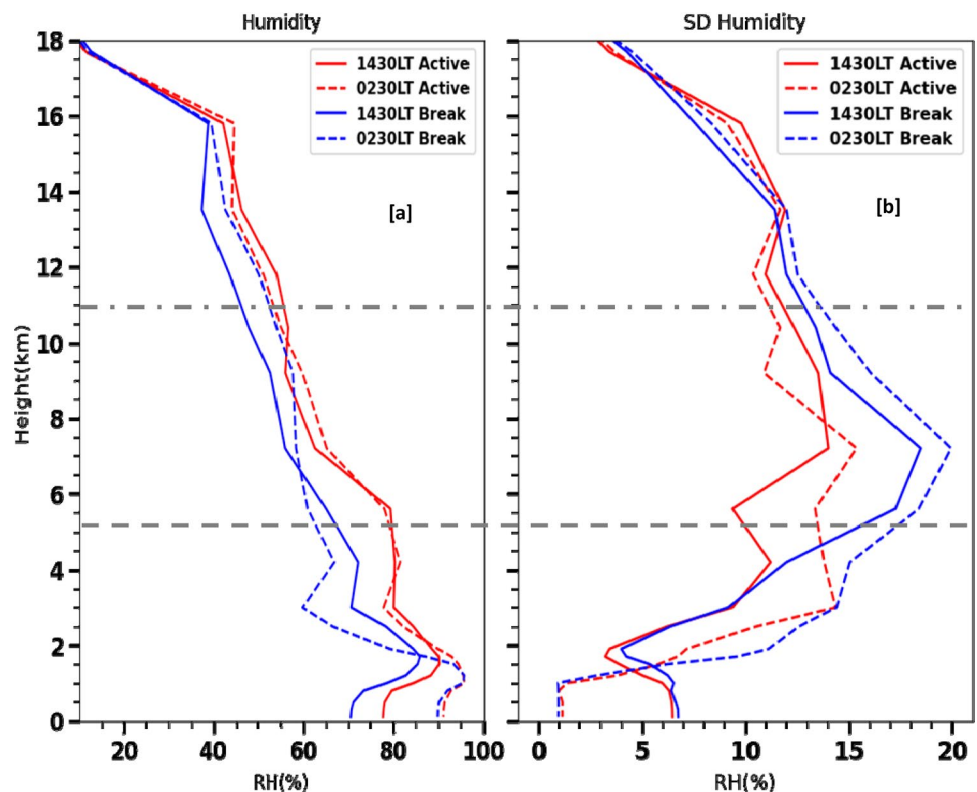


Fig. 12 Complemented composite of humidity profiles for **a** mean and **b** standard deviation over radar site using Indian IMDAA reanalysis (at $3 \times 3^\circ$). It confirms all time high humidity in lower levels below 2 km during ISM. Mid-level, 3–9 km, shows large standard deviations with humidity values occurring above 2.5 km altitude relatively high during night profiles



altitude increases during late afternoon and mid-night (1700–0200 LT), indicating enhanced convective activity. This result is similar to the findings of Liu et al. (2008), which showed that over land, low clouds (> 3.5 km) occurrence is more during day time and above that mid- and high clouds occurrence from 4–14 km are more frequent at 0130 LT. The basic features of less frequency at the mid-level region and a wide range of dBZ_e at the low level during active days remain the same in both the CPR and KaSPR retrieved CFADs at and around 1330 LT (Figs. 11c and 13b). In fact, both CFADs show the maximum occurrence of Z_e at 0 dBZ_e at the warm phase cloud region. Again, similar structural features are found in CPR, and KaSPR retrieved CFADs at and around 0130 LT. Both the CFADs during night time depict the increasing contribution of mid-level cloud region with the low-level peak at higher dBZ_e compared to day time maximum. Since CPR is more sensitive to non-rainy clouds compared to KaSPR, which is more occurring during break ISM days, break days CFADs show some differences both at the day and night times. Although the KaSPR CFAD during break days, when composited for all the hours, shows similar primary and secondary peaks as in CPR CFADs (not shown here). Please note that the obvious difference exists between KaSPR (zenith) and CPR (nadir) comparison due

to the pointing to swath area and time and height sampling differences.

4 Summary and conclusion

The main objective of this study is to document the differences of the VSC through the cloud's macro-physical and microphysical properties during the monsoon active and break spell. CloudSat data for nine years (2008–2016) has been utilized over eight different regions during ISM. Overall summary of VSC over eight regions pertinent to active and break ISM can be seen in Table 3.

During the active period, fully developed VSC due to convective activity is observed over the WI, CI, CE, and NW. It indicated the established state of the monsoon trough over the monsoon core region. Over the NI and SI, broken VSC is observed due to the absence of monsoonal activity and supportive wind patterns over these regions. Developed VSC with deep convection during the break period is observed over the WB and EI regions. It is due to the establishment of a monsoon trough to the foothills of the Himalayas. Due to this movement of the trough to the north of the monsoon core region, clouds of smaller vertical development up to

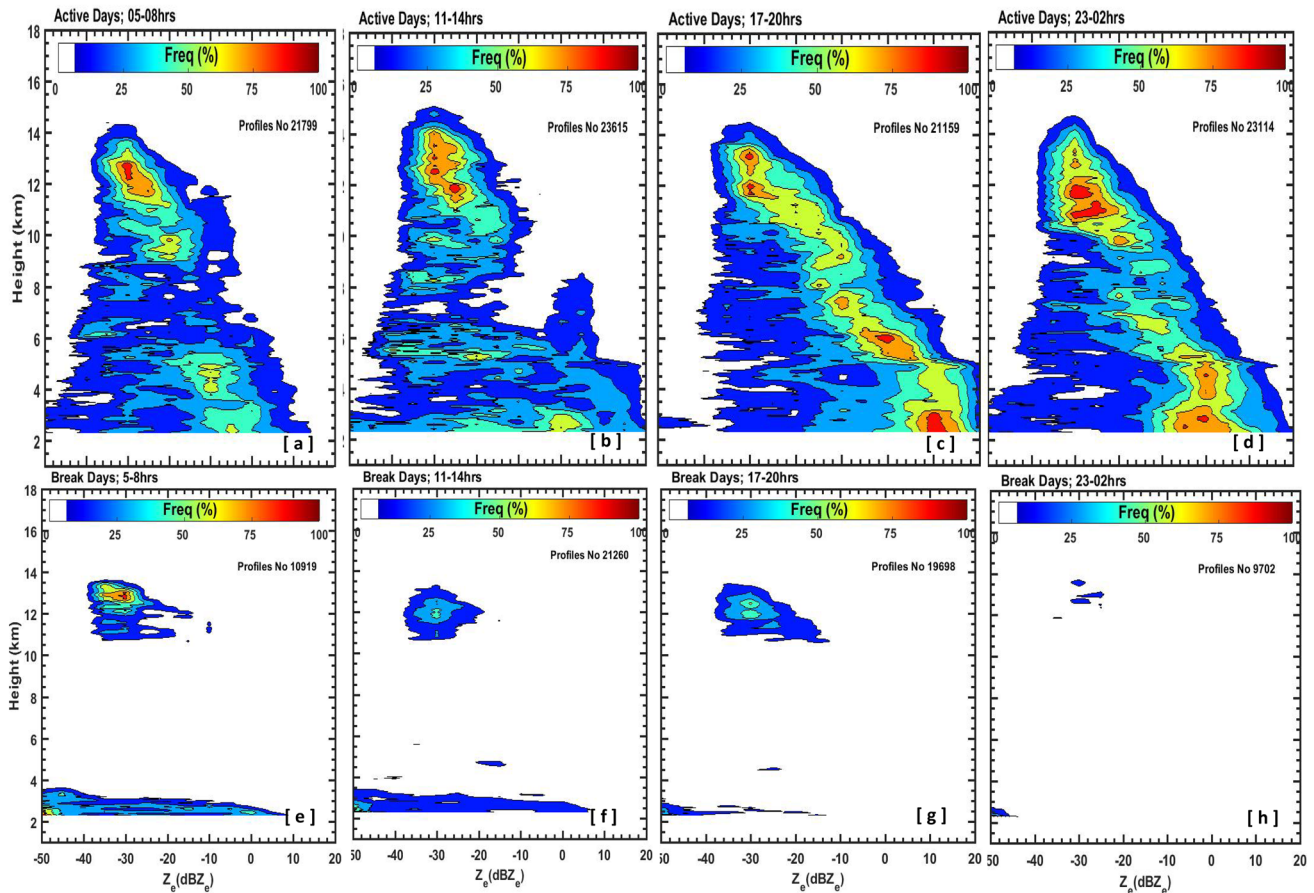


Fig. 13 CFAD of KaSPR Z_e a–d at 05–08, 11–14, 17–20, 23–02 LT, respectively, for active–h break ISM (Jul and Ag) days of 2014

5 km are observed over the core monsoon region and WI. Thermal lows cause the development of shallow convection over the core monsoon region. The most drastic change in the VSC is seen over central to the southwestern part of India during the monsoon active and break spells. Over these regions, during break spells, discontinuity is seen at mid-tropospheric altitude. Hence it is argued here that mid-tropospheric humidity is important to control the local onset of monsoon rains.

Analysis of cloud types suggests that during both spells of ISM, mainly three types of clouds at mid-level (Ac and As) and high level (Ci) show a higher percentage of the occurrence. It is observed that WB and EI regions show accumulative higher cloud frequency. It is due to the availability of the maritime environment and the frequent formation of transient synoptic-scale disturbances nearby these regions. During the active (break) period, As, Ns and Ac clouds have higher frequency over WI, NW, and CI (NI, WB, and EI) regions. Hence, As, Ns, and Ac cloud occurrence shows a higher correlation with the active and break period of monsoon.

Analysis of the microphysical properties of clouds shows significant changes in association with intra-seasonal variability. Irrespective of the active and break spell, LWC shows the highest (lowest) values over WI (NW). Below 3 km, the pattern of LWC profiles over WI is almost the same during active and break days, explaining the similar percentage of Sc cloud occurrence. WB and EI regions show a fairly similar occurrence of LWC during both monsoonal spells. IWC is observed maximum over CE due to the spreading of anvils of deep clouds forming over BoB by tropical easterly jet. The lowest values of IWC are observed over WI, CI, and NW during the ISM break periods due to suppression of convection. Analysis for IER and INC concludes that larger-sized ice hydrometeors ($> 25 \mu\text{m}$) are present at 5–6 km, and their size decreases with altitude. It is also noted that larger-sized hydrometeors ($> 25 \mu\text{m}$) above freezing level show a good correlation with the ISM active and break spells. It indicates that the mixed-phase cloud process plays an important role during ISM. This is similar to the previous studies done in the Indian region.

Here, it is concluded that over the Indian region, the role of the mid-tropospheric clouds (As and Ac) should be

Table 3 Summary on key comparative outcomes of the eight regions pertinent to active and break ISM spells. CH means cloud height extent

Region	Active period	Break period
NI (30°N)	VSC Discontinuous (CH ~ 15 km) Less moisture mid-level (RH < 75% at 600 hPa) due to the established state of monsoon trough away from this region Minimum occurrence of Ns and absence of Dc	VSC continuous (CH ~ 9 km) Dominating warm cloud region. Missing cold cloud region. Mid and upper tropospheric dryness (RH < 40% at 300 hPa) Higher frequency of As, Ns, and Ac
EI (28°N)	VSC mostly continuous (CH ~ 14.5 km) Mid level cloud more dominating All Cloud types: less frequent compared to Break Periods	VSC continuous (CH ~ 14.5 km) Northward propagation of monsoon trough generated over head BoB Higher frequency of As, Ns, and Ac
NW (27°N)	VSC Continuous (CH 17 km) Maximum Z_e (10 dBZ _e) above 10 km due to strong convective updrafts owing to heat low Higher frequency of As, Ns, and Ac. high total cloud amount than break. Minimum LWC	VSC discontinuous (CH ~ 16 km) Total cloud amount is less Minimum LWC
WB (25°N)	VSC Continuous (CH ~ 16 km) Dominating low-level cloud region All Cloud types: less frequent compared to Break Periods	VSC Continuous (CH ~ 16 km) High cloud more occurring Higher frequency of As, Ns, and Ac
CI (24°N)	VSC Continuous (CH ~ 16 km) Dominating warm and mixed phased cloud regions. Higher frequency count of high Z_e centred in the mixed phase region between 4–11 km. Higher frequency of As, Ns, and Ac. high total cloud amount	VSC discontinuous (CH ~ 16 km) Low dBZ _e low cloud and high cloud more occurring Cu more dominating. Complete missing of Ns and Dc
CE (20°N)	VSC Continuous (CH ~ 16.5 km) Dominating warm and mixed phased cloud regions. Higher frequency count of high Z_e centred in the mixed phase region between 4–11 km Dc and Cu more dominating ⁺ . Total cloud amount: no difference between active and break periods	VSC discontinuous (CH ~ 16.5 km) High cloud region more dominating Ci, As, Ns more dominating. Total cloud amount: no difference between active and break periods
WI (18°N)	VSC Continuous (CH 15 km) Dominating 3 levels. Higher frequency count of high Z_e centred in the mixed phase region between 4–11 km Higher frequency of As, Ns, and Ac. Total cloud amount is high Maximum* LWC. Inadequate low level moisture supply from Arabian Sea	VSC discontinuous (CH ~ 14.5 km) High cloud region more dominating Maximum LWC. Inadequate low level moisture supply from Arabian Sea *Maximum refers to comparing among all the selected studied regions for that period +Dominating refers to comparing only that particular study region
SI (12°N)	VSC discontinuous (CH ~ 14 km) due to the absence of monsoonal activity and supportive wind patterns High cloud occurrence from 6–14 km: Advection cirrus clouds from convection centre. The absence of low clouds: do not contribute to ISM rain Only presence of As and Ac (minimum) and Ci	VSC mostly continuous (CH ~ 14 km) High cloud region more dominating Dc and Ci dominating

better represented in the models. During the break periods, mid-tropospheric drying is the main reason behind the suppression of precipitation over India's core monsoon region and southwestern regions. It is well known that the precipitation process generated from the ice or mixed-phase processes needed better representation in the models to get better predictions. The observation in this study offers valuable insights into the relationship between VSC and cloud types with precipitation. However, our analysis is bound by the local time sampling of CloudSat. For finer details of other cloud features, viz. complete diurnal cycle and averages, a synergy of geostationary and ground-based observations is required.

Acknowledgements IITM is an autonomous organization that is fully funded by MOES, Govt. of India. The authors are thankful to the Director of IITM, for every support and help on this research work. The authors are highly indebted to Dr. Jeevanprakash R Kulkarni for his feedback on the initial draft, discussions, and encouragement. Mr. C. Ameya Manas helps in coding extensive data, and the suggested corrective measures are highly appreciated. We are equally grateful to the CloudSat team for data portal help.

Data Availability The CloudSat data used in this study is available at <https://www.cloudsat.cira.colostate.edu/data-products>. For the KaSPR data, please contact the corresponding author (kalapureddy1@gmail.com).

References

- Austin RT, Heymsfield AJ, Stephens GL (2009) Retrieval of ice cloud microphysical parameters using the CloudSat millimetre wave radar and temperature. *J Geophys Res Atmos* 114:D8
- Baker MB (1997) Cloud microphysics and climate. *Science* 276(5315):1072–1078
- Das S, Maitra A, Shukla AK (2011) Melting layer characteristics at different climatic conditions in the indian region: ground based measurements and satellite observations. *Atmos Res* 101(1–2):78–83
- Das SK, Uma KN, Konwar M, Raj PE, Deshpande SM, Kalapureddy MCR (2013) CloudSat–CALIPSO characterizations of cloud during the active and the break periods of indian summer monsoon. *J Atmos Solar Terr Phys* 97:106–114
- Fujinami H, Yasunari T, Morimoto A (2014) Dynamics of distinct intraseasonal oscillation in summer monsoon rainfall over the Meghalaya–Bangladesh–western Myanmar region: covariability between the tropics and mid-latitudes. *Clim Dyn* 43(7–8):2147–2166
- Gadgil S (2018) The monsoon system: land–sea breeze or the ITCZ? *J Earth Syst Sci* 127(1):5
- Gadgil S, Sajani S (1998) Monsoon precipitation in the AMIP runs. *Clim Dyn* 14(9):659–689
- Gambheer AV, Bhat GS (2001) Diurnal variation of deep cloud systems over the indian region using INSAT-1B pixel data. *Meteorol Atmos Phys* 78(3–4):215–225
- Goswami BN, Mohan RA (2001) Intraseasonal oscillations and interannual variability of the indian summer monsoon. *J Clim* 14(6):1180–1198
- Goswami BN, Xavier PK (2005) Dynamics of “internal” interannual variability of the indian summer monsoon in a GCM. *J Geophys Res Atmos* 110:D24
- Houze RA, Wilton DC, Small BF (2007) Monsoon convection in the himalayan region as seen by the TRMM Precipitation Radar. *Q J R Meteorol Soc* 133(627):1389–1411
- Hunt KM, Fletcher JK (2019) The relationship between indian monsoon rainfall and low-pressure systems. *Clim Dyn* 53(3):1859–1871
- Jiang X, Waliser DE, Li JL, Woods C (2011) Vertical cloud structures of the boreal summer intraseasonal variability based on CloudSat observations and ERA-interim reanalysis. *Clim Dyn* 36(11–12):2219–2232
- Johansson E, Devasthale A, L’Ecuyer T, Ekman AM, Tjernström M (2015) The vertical structure of cloud radiative heating over the indian subcontinent during summer monsoon. *Atmos Chem Phys* 15(20):11557–11570
- Johnson RH, Rickenbach TM, Rutledge SA, Ciesielski PE, Schubert WH (1999) Trimodal characteristics of tropical convection. *J Clim* 12(8):2397–2418
- Joseph PV, Sijikumar S (2004) Intraseasonal variability of the low-level jet stream of the asian summer monsoon. *J Clim* 17(7):1449–1458
- Kalapureddy MCR, Sukanya P, Das SK, Deshpande SM, Pandithurai G, Pazamany AL, Annam S (2018) A simple biota removal algorithm for 35 GHz cloud radar measurements. *Atmos Meas Tech* 11(3):1417–1436
- Krishnamurti TN, Ardanuy P (1980) 10- to 20-day westward propagating mode and “Breaks in the Monsoons”. *Tellus* 32:15–26
- Krishnamurti TN, Bhalme HN (1976) Oscillations of a monsoon system. Part I. Observational aspects. *J Atmos Sci* 33(10):1937–1954
- Krishnamurti TN, Thomas A, Simon A, Kumar V (2010) Desert air incursions, an overlooked aspect, for the dry spells of the indian summer monsoon. *J Atmos Sci* 67(10):3423–3441
- Liu C, Zipser EJ, Mace GG, Benson S (2008) Implications of the differences between daytime and nighttime CloudSat observations over the tropics. *J Geophys Res* 113:D00A04. <https://doi.org/10.1029/2008JD009783>
- Medina S, Houze RA Jr, Kumar A, Niyogi D (2010) Summer monsoon convection in the himalayan region: terrain and land cover effects. *Q J R Meteorol Soc* 136(648):593–616
- Mooley DA, Shukla J (1989) Main features of the westward-moving low pressure systems which form over the indian region during the summer monsoon season and their relation to the monsoon rainfall. *Mausam* 40(2):137–152
- Patade S, Shete S, Malap N, Kulkarni G, Prabha TV (2016) Observational and simulated cloud microphysical features of rain formation in the mixed phase clouds observed during CAIPEEX. *Atmos Res* 169:32–45
- Qian Y, Long CN, Wang H, Comstock JM, McFarlane SA, Xie S (2012) Evaluation of cloud fraction and its radiative effect simulated by IPCC AR4 global models against ARM surface observations. *Atmos Chem Phys* 12(4):1785–1810
- Rajeevan M, Gadgil S, Bhate J (2010) Active and break spells of the indian summer monsoon. *J Earth Syst Sci* 119(3):229–247
- Rajeevan M, Rohini P, Kumar KN, Srinivasan J, Unnikrishnan CK (2013) A study of vertical cloud structure of the indian summer monsoon using CloudSat data. *Clim Dyn* 40(3–4):637–650
- Rao TN, Uma KN, Satyanarayana TM, Rao DN (2009) Differences in draft core statistics from the wet to dry spell over Gadanki, India (13.5° N, 79.2° E). *Mon Weather Rev* 137(12):4293–4306
- Rind D, Rossow WB (1984) The effects of physical processes on the Hadley circulation. *J Atmos Sci* 41(4):479–507
- Sathyamoorthy V, Pal PK, Joshi PC (2004) Influence of the upper-tropospheric wind shear upon cloud radiative forcing in the asian monsoon region. *J Clim* 17(14):2725–2735
- Sato T, Kimura F (2007) How does the tibetan Plateau affect the transition of indian monsoon rainfall? *Mon Weather Rev* 135(5):2006–2015
- Subrahmanyam KV, Kumar KK (2017) CloudSat observations of multi layered clouds across the globe. *Clim Dyn* 49:327–341. <https://doi.org/10.1007/s00382-016-3345-7>
- Sukanya P, Kalapureddy MCR (2019) Cloud microphysical profile differences pertinent to monsoon phases: inferences from a cloud radar. *Meteorol Atmos Phys* 131(6):1723–1738
- Sukanya P, Kalapureddy MCR (2021) Cloud radar observations of multi-scale variability of cloud vertical structure associated with indian summer monsoon over a tropical location. *Clim Dyn* 56(3):1055–1081
- Wang J, Rossow WB (1998) Effects of cloud vertical structure on atmospheric circulation in the GISS GCM. *J Clim* 11(11):3010–3029
- Wang B, Kang IS, Lee JY (2004) Ensemble simulations of asian–australian monsoon variability by 11 AGCMs. *J Clim* 17(4):803–818
- Weare BC (2000) Insights into the importance of cloud vertical structure in climate. *Geophys Res Lett* 27(6):907–910
- Webster PJ, Magana VO, Palmer TN, Shukla J, Tomas RA, Yanai MU, Yasunari T (1998) Monsoons: processes, predictability, and the prospects for prediction. *J Geophys Res Oceans* 103(C7):14451–14510
- Yuter S, Houze R (1995) Three-dimensional kinematic and microphysical evolution of Florida Cumulonimbus. Part I: spatial distribution of Updrafts, downdrafts, and precipitation. *Mon Weather Rev* 123(7):1921–1940
- Zhang J, Li Z, Chen H, Yoo H, Cribb M (2014) Cloud vertical distribution from radiosonde, remote sensing, and model simulations. *Clim Dyn* 43(3):1129–1140
- Zuidema P (2003) Convective clouds over the Bay of Bengal. *Mon Weather Rev* 131(5):780–798

- Deng J, Qiu Y, Chen Y, Yang L, He Q, Zhang P (2014) The vertical distribution of ice particle effective radius of clouds and its correlation with precipitation during heavy rainfalls. *J Nat Disasters*. 23:120–128. <https://doi.org/10.13577/j.jnd.2014.0216>
- Goswami BN, Ajayamohan RS, Xavier PK, Sengupta D (2003) Clustering of synoptic activity by indian summer monsoon intraseasonal oscillations. *Geophys Res Lett* 30(8)
- L'Ecuyer TS, Jiang JH (2011) Touring the atmosphere aboard the A-Train. In: AIP Conference Proceedings, vol 1401, no. 1, pp 245–256. AIP
- Rajeevan M, Nanjundiah RS (2009) Coupled model simulations of twentieth century climate of the indian summer monsoon. In: Platinum Jubilee Special Volume of the Indian Academy of Sciences, 537–568
- Rao YP (1976) Southwest Monsoon. In: Meteorological Monograph (Synoptic Meteorology), No.1/1976. India Meteorological Department, New Delhi, p 366
- Sassen K, Wang Z (2008) Classifying clouds around the globe with the CloudSat radar: 1-year of results. *Geophys Res Lett* 35(4)
- Sikka DR (1978) Some aspects of the life history, structure and movement of monsoon depressions. In: Monsoon dynamics. Birkhäuser, Basel, pp 1501–1529
- Subrahmanyam KV, Kumar KK (2013) CloudSat observations of cloud-type distribution over the indian summer monsoon region. In: *Annales Geophysicae*, vol 31. Copernicus GmbH, p 1155. 7
- Stephens GL, Vane DG, Tanelli S, Im E, Durden S, Rokey M, L'Ecuyer T (2008) CloudSat mission: performance and early science after the first year of operation. *J Geophys Res Atmos* 113(D8)
- Webster PJ (1986) The elementary monsoon. In: Monsoons, 3. Monsoons, Wiley, New York, 1987, 3–32
- Wood N (2008) Level 2B radar-visible optical depth cloud water content (2B-CWC-RVOD) process description document. Version 5 1-26
- Zhang J, Chen H, Li Z, Fan X, Peng L, Yu Y, Cribb M (2010) Analysis of cloud layer structure in Shouxian, China using RS92 radiosonde aided by 95 GHz cloud radar. *J Geophys Res Atmos* 115(D7)

Publisher's Note Springer Nature remains neutral with regard to jurisdictional claims in published maps and institutional affiliations.

Springer Nature or its licensor (e.g. a society or other partner) holds exclusive rights to this article under a publishing agreement with the author(s) or other rightsholder(s); author self-archiving of the accepted manuscript version of this article is solely governed by the terms of such publishing agreement and applicable law.